

# M2M X-Hab 2021 Academic Innovation Challenge

## Thermal Radiator for CO<sub>2</sub> Deposition in Deep Space Transit

The University of North Texas

X-Hab Team: Travis Seaver, Eric Lira, Jesus De La Torre, Anthony Pezzulli, Balmore Giron

Faculty Mentors: Dr. Huseyin Bostanci (PI), Dr. Cable Kurwitz (Co-PI, Texas A&M University)

Final Report

August 2021

# Table of Contents

<b>TABLE OF CONTENTS</b> .....	<b>2</b>
LIST OF FIGURES.....	4
LIST OF TABLES.....	5
<b>EXECUTIVE SUMMARY</b> .....	<b>6</b>
<b>1. INTRODUCTION</b> .....	<b>7</b>
1.1. OBJECTIVE.....	7
1.2. MOTIVATION .....	7
1.3. APPROACH .....	7
<b>2. PROJECT TIMELINE</b> .....	<b>8</b>
2.1. QUARTER 1 (Q1).....	8
2.2 QUARTER 2 (Q2).....	8
2.3 QUARTER 3 (Q3).....	8
2.4 QUARTER 4 (Q4).....	9
<b>3. DESIGN EVOLUTION</b> .....	<b>10</b>
3.1. SUMMARY OF COMPETITIVE DEVELOPMENTS .....	10
3.2.1 PHASES OF THE PROJECT DESIGN .....	11
3.2.2 RE-DESIGN TO ACCOMMODATE MORE AVAILABLE COMPONENTS .....	13
3.3. ANALYSIS .....	15
3.4. SAFETY CONSIDERATIONS .....	21
3.5. ETHICAL/PROFESSIONAL CONSIDERATIONS .....	24
3.6. ESTIMATED LIFE CYCLE OF DEVELOPMENT .....	25
3.7. COST BREAKDOWN OF DEVELOPMENT .....	25
<b>4. FABRICATION</b> .....	<b>28</b>
4.1. FABRICATION METHODS.....	28
4.2. FABRICATION STAGES .....	30
<b>5. TESTING</b> .....	<b>33</b>
5.1. TESTING PLAN .....	33
5.2. INSTRUMENTATION AND DATA ACQUISITION .....	33
5.3. RESULTS.....	34
5.4. CONCLUSIONS .....	35
5.5. ADDITIONAL WORK DONE DURING SUMMER 2021.....	35
<b>6. MARKETING PLAN</b> .....	<b>37</b>
6.1. PROJECT LOGO .....	37
6.2. BROCHURE .....	38
6.3. TARGET MARKET .....	40
6.4. MEANS OF ACCESSING THE TARGET MARKET .....	40
<b>7. TEAM PERSONNEL</b> .....	<b>41</b>
7.1. TEAM PERSONNEL RESPONSIBILITIES.....	41
7.2. RESUMES .....	42
<b>APPENDIX A:</b> .....	<b>47</b>
REFERENCES .....	47

<b>APPENDIX B:</b> .....	<b>49</b>
COMPLETE SPECIFICATIONS FOR MAJOR PURCHASED PARTS/COMPONENTS .....	49
<b>APPENDIX C:</b> .....	<b>50</b>
DRAWINGS FOR CUSTOM-BUILT OR FABRICATED PARTS/COMPONENTS/SUB-ASSEMBLIES .....	50
<b>APPENDIX D:</b> .....	<b>51</b>
BILL OF MATERIALS .....	51
<b>APPENDIX E:</b> .....	<b>53</b>
FEA PARAMETERS ITERATIVE ANALYSIS.....	53

## List of Figures

FIGURE 1: LITHIUM HYDROXIDE CANNISTER [3] .....	10
FIGURE 2: CDRA FROM THE ISS [3] .....	11
FIGURE 3: INITIAL PROPOSAL SCHEMATIC.....	11
FIGURE 4:PROTOTYPE REV 1 SCHEMATIC .....	12
FIGURE 5:PROTOTYPE REV 2 SCHEMATIC .....	12
FIGURE 6:PROTOTYPE REV 3 SCHEMATIC .....	12
FIGURE 7 SCHEMATIC OF FINAL DESIGN, INCLUDING PRE-HEATER & PRE-CHILLER.....	14
FIGURE 8 CAD MODEL OF FINAL DESIGN .....	14
FIGURE 9: PYTHON CODE FOR PLOTTING PANEL SIZE.....	16
FIGURE 10: RELATIONSHIP OF AREA, TEMP, AND Q .....	16
FIGURE 11: SINGLE-ROW PIPING CONFIG. REDISTRIBUTED.....	17
FIGURE 12: PYTHON CODE FOR THERMAL RESISTANCE .....	18
FIGURE 13: PLOT FOR SERIES AND PARALLEL THERMAL RESISTANCE.....	18
FIGURE 14 SOLIDWORKS FEA CAPTURE MODE .....	19
FIGURE 15 SOLIDWORKS FEA RECOVERY MODE .....	19
FIGURE 16: SAFETY FLOW-DOWN .....	21
FIGURE 17 TUBE BENDER .....	28
FIGURE 18 SHEET METAL BENDER .....	28
FIGURE 19 BRAZING USING SILVER ALLOY ROD.....	29
FIGURE 20 SHEET METAL SHEAR [21].....	29
FIGURE 21 RIDGID™ PIPE CUTTER .....	30
FIGURE 22 CUTTING ALUMINUM HONEYCOMB .....	30
FIGURE 23 DUAL PANEL RADIATOR JOINING & ASSEMBLY .....	31
FIGURE 24 BRAZING FITTINGS TO THE PIPING SYSTEM .....	31
FIGURE 25 FINISHED PLUMBING AFTER BRAZING & BENDING.....	31
FIGURE 26 FULLY ASSEMBLED SYSTEM, POST-LEAK-CHECK, PRIOR TO DAQ INTEGRATION .....	32
FIGURE 27 FULLY ASSEMBLED SYSTEM, INTEGRATED WITH DAQ, PRIOR TO TESTING; 1) PUMP, 2) RESERVOIR, 3) AIR LINE FOR PURGING SYSTEM, 4) FLOW METER, 5) POWER SUPPLY UNIT FOR PUMP, 6) DUAL-PANEL RADIATOR, 7) DAQ .....	32
FIGURE 28 WEIGHING WATER TO FIND VOLUME, COMPARING TO OUTPUT OF FLOW METER .....	34
FIGURE 29 SCREEN CAPTURE OF THE DAQ WITH SYSTEM ON .....	34
FIGURE 30 AIR PURGING THE SYSTEM & TURNING SYSTEM TO "CAPTURE" MODE .....	35
FIGURE 31 PRELIMINARY TESTING OF RADIATOR PROTOTYPE IN CAPTURE MODE.....	36
FIGURE 32 PRELIMINARY TESTING OF RADIATOR PROTOTYPE IN RECOVERY MODE .....	36
FIGURE 33 TRI-FOLD BROCHURE, INSIDE .....	38
FIGURE 34 TRI-FOLD BROCHURE, OUTSIDE .....	39

## List of Tables

TABLE 1 PUMP COMPARISON .....	13
TABLE 2: RISKS, CONSEQUENCES, AND MITIGATION APPROACH .....	22
TABLE 3: OSHA HAZ COMM STANDARDS .....	24
TABLE 4: HUMAN SAFETY RISKS, CONSEQUENCES, MITIGATION APPROACH.....	24
TABLE 5: BILL OF MATERIALS .....	27
TABLE 6 FLOW METER CALIBRATION/TESTING .....	33
TABLE 7: EDUCATIONAL OUTREACH POC'S .....	40

## EXECUTIVE SUMMARY

*This UNT Senior design team was tasked by NASA to develop a variable conductance thermal radiator prototype for CO<sub>2</sub> deposition for deep space transit. NASA selects university teams every year to partake in the X-HAB Academic Innovation Challenge, with this year's number of teams being six. Air Revitalization is a crucial system for any space travel, be it for Low Earth Orbit, such as the International Space Station, or for deep space transit. Current systems, such as the Carbon Dioxide Removal Apparatus aboard the ISS, require upkeep and maintenance, which cannot be done on long distance space missions. For the past several years, NASA has done research on Cryogenic systems for Carbon Dioxide removal. These systems operate on the fact that Carbon Dioxide freezes at a higher temperature than Oxygen and Nitrogen, so Carbon Dioxide can be frozen out of the cabin atmosphere without the use of filters, which degrade over time. To cool the cabin air down to a temperature where Carbon Dioxide freezes, Stirling cryocoolers have been used, which have shown promise in the hope of Carbon Dioxide deposition for Cabin Air Revitalization. Cryogenic systems are much more reliable but require significant energy input to operate. Physical systems, such as radiators, have generally not been used for this task, as there is a need to be able to "turn off" the rejection of heat to allow the frozen carbon dioxide to be collected. However, with working fluids pumped through a physical radiator, that aspect of operation can be achieved. The goal of this challenge is to determine the effectiveness of a variable conductance thermal radiator that can reject heat to deep space, without the use of a dedicated cryocooler to remove energy from the cabin air. The proposed design uses piping, hot and cold working fluids, and non-condensable gas to absorb heat from the cabin air on one side of the radiator and reject the heat to deep space by means of thermal radiation. As well, the system will allow for the recovery of deposited Carbon Dioxide. The UNT X-HAB 2021 team will create a model radiator and test its performance with simulated heat sources and sinks and extrapolate those data points to analyze for real world conditions.*

# 1. INTRODUCTION

An estimated 400,000 individuals were involved in making the Apollo Missions successful during the 1960's. [1] This figure includes everyone from astronauts to caterers: thousands of engineers, scientists, mathematicians, medical personnel, and programmers. They were individuals of different races, ethnicities, socio-economic backgrounds, and creeds, who came together with common purpose and unmatched resolve to land 12 men on the moon. The portmanteau *university* stems from the Latin word *universitas*, meaning whole or together, and the English word *diversity*. Fitting then, that NASA has once again turned to an army of diverse individuals to carry on the tradition and mission of the Apollo program of propelling mankind into the stars. The upcoming deep space missions will require a tremendous breadth and depth of technology in order to successfully put man on the Moon again, as well as on Mars. NASA has selected several universities across the US, including the University of North Texas, this year to work on developing solutions to a wide range of deep space transit challenges, from food production to air revitalization.

## 1.1. Objective

Our objective for this NASA Moon-to-Mars X-Hab Academic Challenge is to design, model, build and test a prototype variable conductance radiator to simulate CO<sub>2</sub> capture and recovery. This prototype will be able to cycle between capture and recovery mode, and will be able to reach a surface temperature of 130K, the temperature needed for the deposition of CO<sub>2</sub>.

## 1.2. Motivation

The current methods of CO<sub>2</sub> capture and recovery are costly in terms of energy usage, manhours spent maintaining the system, weight, consumable resources, and replacement part cost. Our motivation is to solve these issues by utilizing the low heat sink temperatures of deep space and waste heat from other systems transferred by fluid in order to produce an efficient way to capture and recover CO<sub>2</sub>.

## 1.3. Approach

Thermal energy always moves from a medium of higher temperature to a medium of lower temperature via conduction (surface-to-surface contact), convection (movement of some kind of fluid), or radiation (the emittance of electromagnetic waves). In order for thermal energy, or heat, to move from one body to another, there must be a temperature gradient. [2] Our approach is to use the temperature gradient between the cabin of a spacecraft (which must be high enough to support human life) and the vast sink of space. By moderating the rate at which thermal energy transfers from dehumidified cabin air to the sink of outer space, we can safely and efficiently reject thermal energy from gaseous CO<sub>2</sub>, thereby creating a phase change from a gaseous to a solid state of matter. Once CO<sub>2</sub> is in solid state, it can be captured and used for other systems on the spacecraft. Under the typical temperatures and pressures found in Earth's atmosphere, CO<sub>2</sub> changes phases from solid form (dry ice) to gaseous form without going through a liquid phase. Each time matter changes phases, a tremendous amount of energy is required. Since CO<sub>2</sub> under these conditions has such a large phase shift, the energy that is released or absorbed is relatively higher than other typical atmospheric gases. We will take advantage of the huge temperature gradient that will exist between the cabin and deep space to accommodate this phase change. However, although this gradient can be advantageous to us, it could also be potentially dangerous. The radiator we will design will need to be able to safely moderate the amount and rate of heat being transferred. We want to reject *only* the amount of heat we need to solidify CO<sub>2</sub>; losing any more than that is energy that will need to be reproduced by other systems. By using carefully calculated fluid dynamics and vacuum insulation, we will predict and control the heat transfer rate from inside to outside.

## 2. PROJECT TIMELINE

The following Gantt Chart shows our planned procedure and timeline for meeting all NASA design reviews. On the left side of the chart, major tasks are highlighted in yellow, with sub-tasks below them. Each light-green event is a checkpoint with NASA, and is denoted by a single date. The timeline is split into quarters. Because this project began in the Fall 2020 semester of UNT, Q1 is from September to November 2020, Q2 is from November to 31 December 2020, Q3 is from 1 January 2021 to mid-March 2021, and Q4 is from mid-March until the end of the Spring 2021 term, 23 April 2021. The timeline portion to the right of the dates is denoted with actual progress (dark green) and projected completion/progress (pale yellow). The timeline is current up to the week of 23 April (present time is denoted by the blue line).

### 2.1. Quarter 1 (Q1)

Level	Description	Start date	End date	13-Sep	20-Sep	27-Sep	4-Oct	11-Oct	18-Oct	25-Oct	1-Nov
1.1.0	Radiator Design	13-Sep-20	7-Oct-20	█	█		█				
1.1.1	Learn, Read, Understand proposal	13-Sep-20	23-Sep-20	█	█						
1.1.2	Kickoff meeting	24-Sep-20			◆						
1.1.3	Learn about NASA expectations and processes	25-Sep-20	7-Oct-20	█	█		█				
1.1.3.1	SDR system architecture, level 1 requirements, WBS	25-Sep-20	7-Oct-20	█	█		█				
1.1.3.2	SDR Preferred System Solution	25-Sep-20	7-Oct-20	█	█		█				
1.1.3.3	SDR functional baseline, ConOps, software reqs	25-Sep-20	7-Oct-20	█	█		█				
1.1.3.4	SDR Risk management, analysis tools, test plans	25-Sep-20	7-Oct-20	█	█		█				
1.1.4	System Definition Review Meeting	8-Oct-20					◆				
1.2.0	Radiator Modeling	9-Oct-20	20-Jan-21					█	█	█	█
1.2.1	Design Variable Conductance Radiator	9-Oct-20	20-Jan-21					█	█	█	█
1.2.1.1	Learn software for modeling	11-Oct-20	25-Oct-20					█	█		
1.2.1.2	Materials Research	18-Oct-20	1-Nov-20						█	█	
1.2.1.3	Determine possible design parameters	25-Oct-20	8-Nov-20							█	█
1.2.2	Preliminary Design Review Meeting	12-Nov-20									
1.2.2.1	Refine design parameters	13-Nov-20	20-Jan-21								
1.2.2.2	Update design and finalize system operations	13-Nov-20	20-Jan-21								

### 2.2 Quarter 2 (Q2)

Level	Description	Start date	End date	8-Nov	15-Nov	22-Nov	29-Nov	6-Dec	13-Dec	20-Dec	27-Dec
1.1.0	Radiator Design	13-Sep-20	7-Oct-20								
1.1.1	Learn, Read, Understand proposal	13-Sep-20	23-Sep-20								
1.1.2	Kickoff meeting	24-Sep-20									
1.1.3	Learn about NASA expectations and processes	25-Sep-20	7-Oct-20								
1.1.3.1	SDR system architecture, level 1 requirements, WBS	25-Sep-20	7-Oct-20								
1.1.3.2	SDR Preferred System Solution	25-Sep-20	7-Oct-20								
1.1.3.3	SDR functional baseline, ConOps, software reqs	25-Sep-20	7-Oct-20								
1.1.3.4	SDR Risk management, analysis tools, test plans	25-Sep-20	7-Oct-20								
1.1.4	System Definition Review Meeting	8-Oct-20									
1.2.0	Radiator Modeling	9-Oct-20	20-Jan-21	█	█	█	█	█	█	█	█
1.2.1	Design Variable Conductance Radiator	9-Oct-20	20-Jan-21	█	█	█	█	█	█	█	█
1.2.1.1	Learn software for modeling	11-Oct-20	25-Oct-20								
1.2.1.2	Materials Research	18-Oct-20	1-Nov-20								
1.2.1.3	Determine possible design parameters	25-Oct-20	8-Nov-20								
1.2.2	Preliminary Design Review Meeting	12-Nov-20		◆							
1.2.2.1	Refine design parameters	13-Nov-20	20-Jan-21								
1.2.2.2	Update design and finalize system operations	13-Nov-20	20-Jan-21	█	█	█	█	█	█	█	█

### 2.3 Quarter 3 (Q3)



Level	Description	Start date	End date	3-Jan	10-Jan	17-Jan	24-Jan	31-Jan	7-Feb	14-Feb	21-Feb	28-Feb	7-Mar
1.2.0	Radiator Modeling	9-Oct-20	20-Jan-21										
1.2.1	Design Variable Conductance Radiator	9-Oct-20	20-Jan-21										
1.2.2.1	Refine design parameters	13-Nov-20	20-Jan-21										
1.2.2.2	Update design and finalize system operations	13-Nov-20	20-Jan-21										
1.2.3	Critical Design Review Meeting	21-Jan-21				◆							
1.3.3	Progress Checkpoint Review Meeting	11-Mar-21											◆
1.3.0	Prototype Fabrication	22-Jan-21											
1.3.1	Build scale prototype radiator												
1.3.2	Gather data from onboard temp/pressure sensors												
1.4.0	Prototype Testing												
1.4.1	Test radiator's functionality												
1.4.2	Test variable conductance capability												
1.5.0	Data Analysis and Reporting												
1.5.1	Analyze Data gathered												
1.5.1.1	Extrapolate data for 1kW heat rejection												
1.6.0	Project Completion and NASA Evaluation	6-May-21											

## 2.4 Quarter 4 (Q4)

Level	Description	Start date	End date	14-Mar	21-Mar	28-Mar	4-Apr	11-Apr	18-Apr	25-Apr	2-May
1.2.0	Radiator Modeling	9-Oct-20	20-Jan-21								
1.2.1	Design Variable Conductance Radiator	9-Oct-20	20-Jan-21								
1.2.2.1	Refine design parameters	13-Nov-20	20-Jan-21								
1.2.2.2	Update design and finalize system operations	13-Nov-20	20-Jan-21								
1.2.3	Critical Design Review Meeting	21-Jan-21									
1.3.3	Progress Checkpoint Review Meeting	11-Mar-21									
1.3.0	Prototype Fabrication	22-Jan-21									
1.3.1	Build scale prototype radiator										
1.3.2	Gather data from onboard temp/pressure sensors										
1.4.0	Prototype Testing										
1.4.1	Test radiator's functionality										
1.4.2	Test variable conductance capability										
1.5.0	Data Analysis and Reporting										
1.5.1	Analyze Data gathered										
1.5.1.1	Extrapolate data for 1kW heat rejection										
1.6.0	Project Completion and NASA Evaluation	6-May-21									◆

Note: 1 Red indicates inability to complete due to system not being fully functional before end of semester

### 3. DESIGN EVOLUTION

The following section details how the design of our radiator changed over time, as well as predecessor systems that have led to current systems being used and future systems in development. The design process is cyclical in nature, and as such this will most likely not include all iterations of design. Currently, we have 4 revisions on the prototype design. In general, the design process includes inception, theoretical analysis, modeling, manufacturing, testing, development, experimental analysis, and then the final design. The process is cyclical in that each subsequent step may cause engineers to restart at a previous step. Most designs go through several iterations of the process before a final design is produced. Several roadblocks forced us to make several changes to the design as well, due to time and budget constraints. These last-minute changes will be discussed below.

#### 3.1. Summary of Competitive Developments

The very first life-support systems for space travel were simple, reliable filtration systems. Honeywell developed the Environmental Control and Life Support system (ECLS) which consisted of LiOH (lithium hydroxide) canisters. The ECLS was used from the Mercury program, through Gemini, and into the Apollo program. The canisters were simple and reliable, but required astronauts to change them out on a routine basis. They were also wasteful in the sense that the CO<sub>2</sub> was captured, but not reused for anything. They also required an abundance of LiOH canisters be carried on mission. This meant they could not be used for long-duration missions. The maximum duration mission this system could be used on was anywhere from 5 to 14 days. [3]



Figure 1: Lithium Hydroxide Cannister [3]

For applications of missions lasting longer than 10 days, Honeywell developed a bed molecular sieve system which used a silica gel to remove both water and CO<sub>2</sub> from cabin air. Other filtration systems based on this designed were developed for use on Skylab and later on the International Space Station (ISS), where a long duration system was required (the ISS is the longest running space mission; it has been running for nearly 20 years and is still ongoing to this day). The current system used in the ISS is the Carbon Dioxide Removal Assembly, or CDRA. Today, CDRA is used in conjunction with an electrolysis system to convert the captured CO<sub>2</sub> back into oxygen. CDRA is currently the standard in CO<sub>2</sub> revitalization technology. However, it still has some issues which our system hopes to address. These issues include pellet contamination of the gels and desiccants used, excessive dust from the pellet beds which can cause issues with computer systems and sensors on board, and shorts of the heating system used in CDRA. [3]

Although CDRA has been reliable onboard the ISS for the last 15 years, it still requires a lot of routine maintenance. The ISS has the convenience of having earth close by for access to replacement parts and routine maintenance parts. However, in deep space transit, spacecraft will not have access to

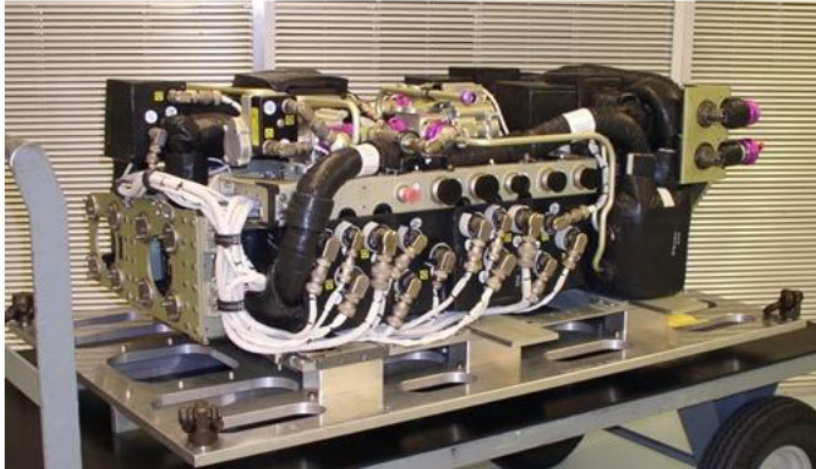


Figure 2: CDRA from the ISS [3]

replacement or maintenance parts. Future Mars missions will require the environmental control systems to work for up to 36 months. [3]

Outside of space applications, there are similar CO<sub>2</sub> recovery systems in use on nuclear submarines. Many of the technologies developed for space travel are used in nuclear submarines. Lithium Hydroxide cannisters are still in use; however, the issues of weight and storage space of both new and used cannisters are less of an issue on submarines, where weight and storage space are not

nearly as much of an issue. [4] In Switzerland, there exists a climate control plant owned by Climeworks AG which sucks carbon dioxide from the air in effort to lower greenhouse gasses planet wide. [5]

Future technologies, that are in development include the different sorbents that reduce the amount of dust produced (such as solid and liquid amines), [3] as well as on-board cryogenic coolers. Cryocoolers are currently used in power plants to scrub CO<sub>2</sub> from flue gas for environmental concerns, [6] but the technology utilizes too much power when scaled up to a size that would accommodate a deep space vehicle. [7]

### 3.2.1 Phases of the Project Design

The initial design for the project was provided by Dr. Huseyin Bostanci of UNT and Dr. Cable Kurwitz of TAMU. This design, shown in Figure 3, was based on a previous NASA JPL design and successfully tested in 2012. [8] This solution is an integration of the NASA JPL radiator along with the proposed air revitalization technology. The design has two radiator panels that alternate in operation; the cold radiator uses space as the sink to cool down to the point that will allow CO<sub>2</sub> to deposit on the surface, while the warm radiator uses waste thermal energy from other parts of the spacecraft transported by the fluid system to capture the solidified CO<sub>2</sub>.

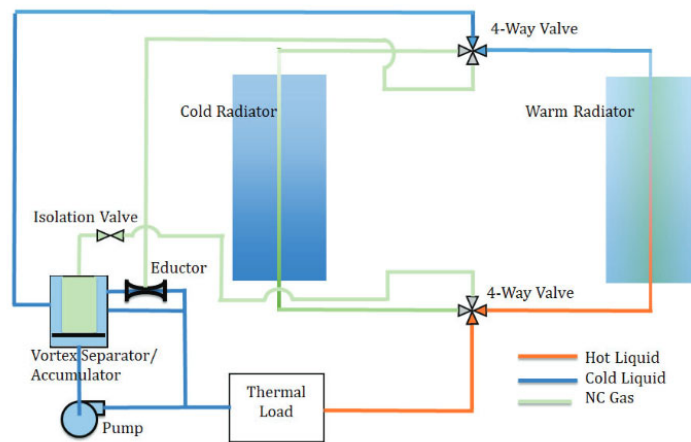


Figure 3: Initial Proposal Schematic

Figure 4 shows how the schematic shown in Fig 3 will operate in a test environment. An electric heater will be used to simulate the deposition of CO<sub>2</sub> on the surface of the cold panel of the radiator. Since

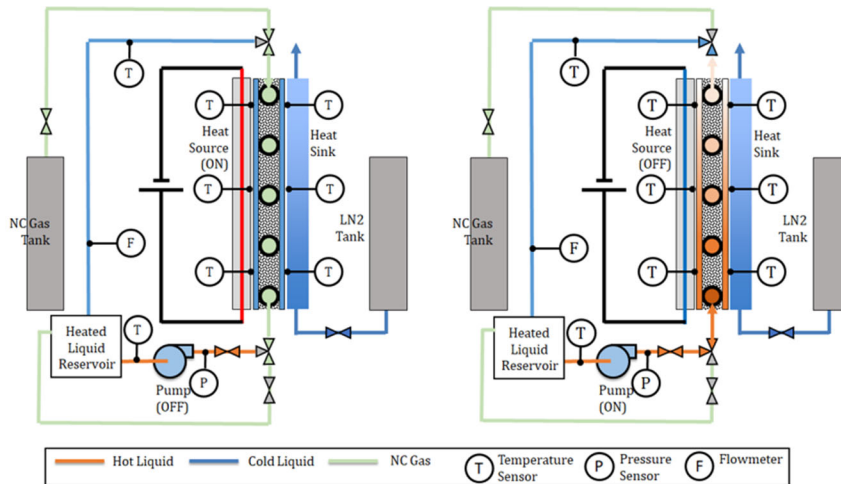


Figure 4: Prototype Rev 1 Schematic

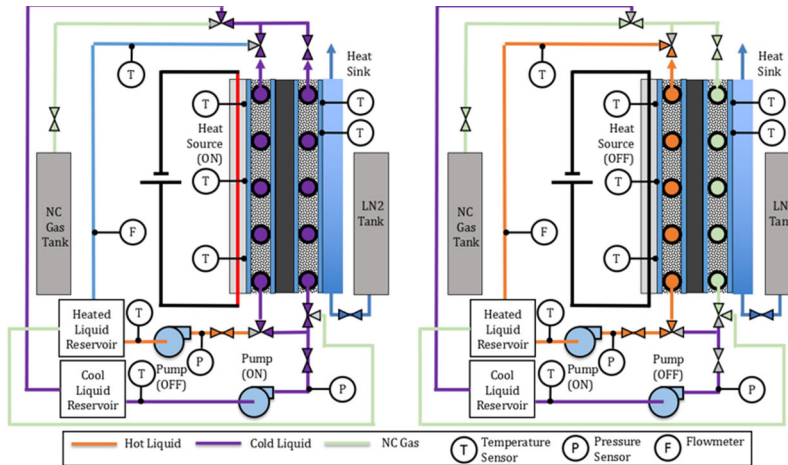


Figure 5: Prototype Rev 2 Schematic

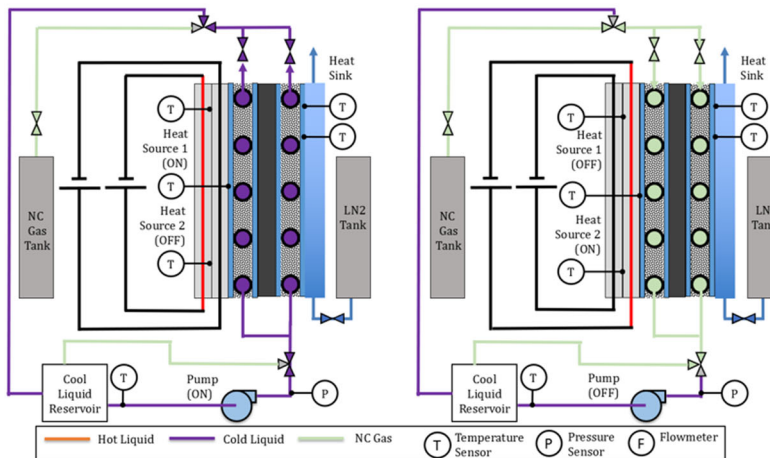


Figure 6: Prototype Rev 3 Schematic

gaseous CO<sub>2</sub> releases a lot of energy when it solidifies into dry ice, that energy will be simulated by electric/thermal energy provided by a heater.

Figure 5 shows the next iteration of the test schematic. In this iteration, the single row of tubing in the radiator pane is replaced with two rows of tubing separated by an insulating vacuum section. This double row of tubes with the vacuum insulation in the center allows us to better control the temperature gradient between the simulated heat sink of space (simulated using liquid nitrogen) and the inner surface of the radiator (simulated by the electric heat source).

Following revision 2, the test schematic was further refined to include a second electric heat source that will simulate the waste thermal load from other on-board systems and transported to the radiator by a fluid capable of handling the temperatures needed.

This next schematic is shown in Figure 6. In order for this prototype to operate, the first heat source will be on during CO<sub>2</sub> capture mode to simulate the deposition of CO<sub>2</sub>. Liquid nitrogen will simulate the heat sink of space. During CO<sub>2</sub> recovery mode, the first heat source will be switched off and the second heat source will be switched on. This second heat source simulates the waste thermal energy from other systems that will be transported to the radiator via liquid cooling system. In a fully operational system, this liquid cooling system would be needed to cool off critical systems such as computers elsewhere on the vehicle. It

would be used as a buffer to control the temperature gradient across the radiator and will also reject any unused waste heat to space.

### 3.2.2 Re-design to Accommodate More Available Components

During our search for a pump that could handle the cryogenic temperatures of boiling liquid nitrogen, we eventually realized that a pump that would satisfy our needs would be out of our budget and would not be able to be delivered before the end of the semester. Several pumps were considered, of various designs. However, none of these would meet our application for various reasons. Typical centrifugal pumps and gear pumps would not be able to withstand the nearly  $-200^{\circ}\text{C}$  temperatures of the working fluids. Rubber & silicon seals and o-rings necessary to keep the system pressurized and keep the pump from leaking get brittle and stop sealing below  $-40^{\circ}\text{C}$ . Because of this, we considered using a liquid nitrogen transfer pump, the same type used to actually fill liquid nitrogen tanks. The main issues with these types of pumps is that they are typically not used to high-pressure applications, and they are not capable of handling liquid propylene working fluid. Three options were considered: the Gowe™, Micromeritics™, and Air Liquide™. The comparison of these pumps is shown in the below table. Gowe™ pump is a manual hand-operated pump, and while it was available on Amazon™ and within our budget, it would have been highly impractical for moving the working fluid through the system, as it would most likely take several hours to allow the system to reach steady state and collect data. The other two pumps considered were electric, and either cost too much or could not arrive in time for testing. Additionally, these style pumps are not meant for high-pressure applications needed to keep propylene a liquid.

The last option considered was to make a venturi ejector pump. This would essentially just use a venturi and the venturi effect to push the liquid propylene through the system. A pressurized canister of liquid propylene would be connected to the system, and a venturi would be placed under the pressure vessel. As the fluid exits the tank, it is accelerated by the venturi and circulates through the system. Flow is regulated by the size of this venturi. This system, while in theory would work, also has several issues. It would require the propylene to be discharged into the atmosphere. Propylene is a highly flammable gas at atmospheric pressure and temperature, so this would pose a serious fire and explosion hazard. In addition, while the parts to make this ejector pump would be inexpensive, the maintenance cost of continuously buying propylene would be very high. Also, the system is wasteful.

<i>Manufacturer</i>	<i>Description</i>	<i>Cost &amp; Lead Time</i>	<i>Issues</i>
Gowe™	Manual operated LN2 transfer pump	\$, 1 month	Operated manually by hand; not practical for several hour-long testing
Micromeritics™	Electric LN2 transfer pump	\$, several months	Too expensive, lead time too long, cannot handle high pressure, cannot handle liquid propylene
Air Liquide™	Electric LN2 transfer pump	\$, several months	Lead time was 6-8 months, made in France
N/A	Venturi Ejector	\$, N/A	Wastes propylene, discharges to atmosphere (cold, liquid propylene going through phase change, dangerous, flammable)

*Table 1 Pump Comparison*

In order to solve this issue in our design, we decided to abandon using liquid nitrogen as a heat sink and using propylene as our working fluid. Instead, we opted to replace boiling liquid nitrogen with an acetone-dry ice bath and replacing our working fluid with acetone. This would reach nearly  $-80^{\circ}\text{C}$  and would provide us a proof of concept for the system. We would be able to see heat transfer and be able to calculate the heat transfer rate & show that the system could work with the right pump. However, even with this design change, we could not find a pump that could handle temperatures below  $-40^{\circ}\text{C}$ . Because of this, we came up with the idea to heat up the working fluid when it exits the radiator & goes into the reservoir, prior to reaching the pump. When the fluid reaches the pump, it would be above  $0^{\circ}\text{C}$ . This gave

us many options for available pumps, and we were able to use one from the UNT Thermal Management Lab. When the fluid leaves the pump, it would be cooled back down to the proper temperature with a secondary acetone-dry ice bath.

In order to make this work, we would need to know how much heat to put into the working fluid to bring it up to around 0°C. The Analysis section below goes into how the length of heat-tape was calculated.

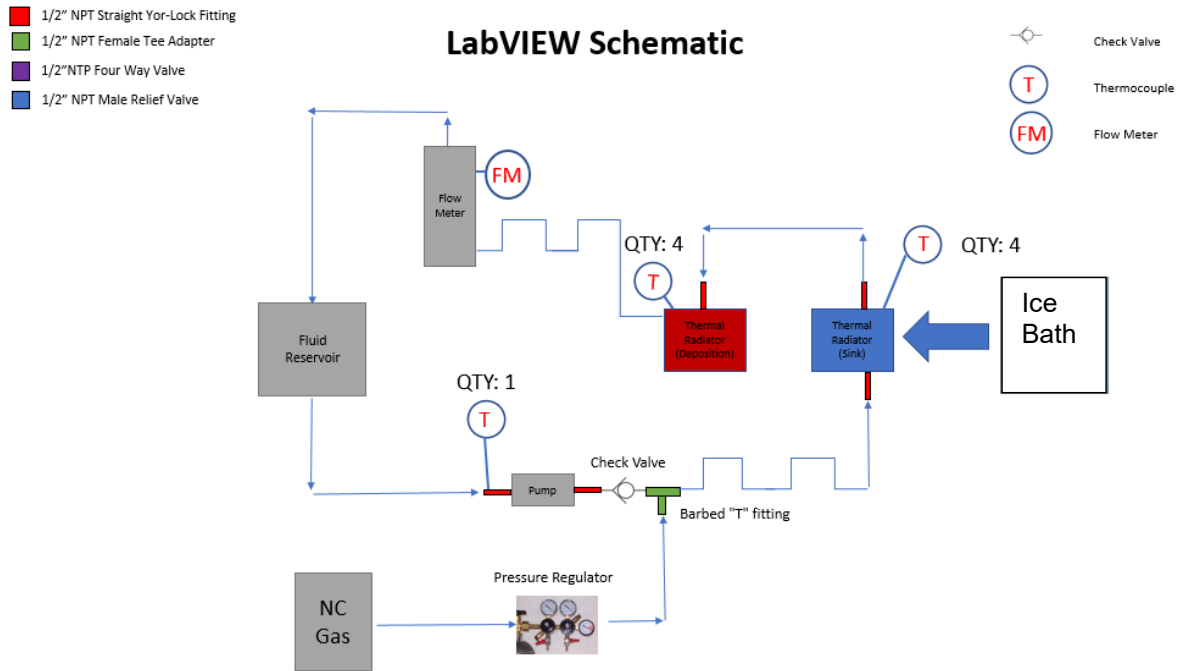


Figure 7 Schematic of final design, including pre-heater & pre-chiller

This LabVIEW Schematic shows the final design of the system. The U-bend represent the pre-heater with the heat tape and the pre-chiller with a secondary ice bath.

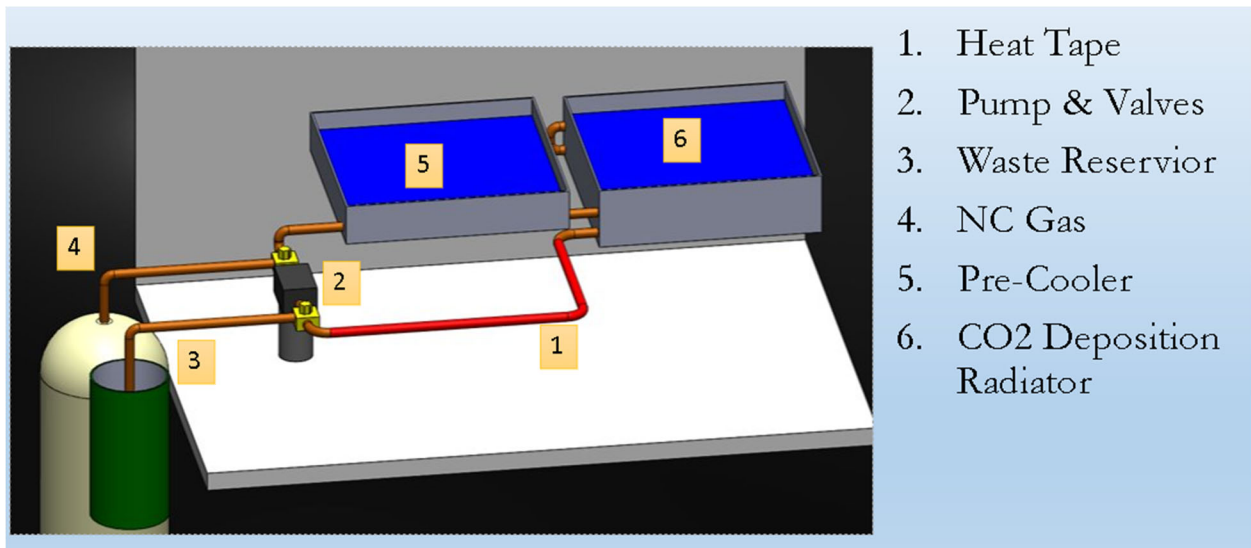


Figure 8 CAD model of final design

### 3.3. Analysis

Our analysis was carried out using Python for numerical analysis, Solidworks FEA, and analytical calculations. We first needed to start with the amount of energy it would take to deposit a typical daily amount of CO<sub>2</sub>. Next, with the aid of Python, we created a model we could later use in the design of the radiator. This model gave us the ability to choose the number and size of pipes inside the radiator panel. Solidworks FEA allowed us to verify that the system would reject the amount of heat we needed it to reject. Finally, various calculations were done to determine the amount of energy to deposit CO<sub>2</sub>, and to determine the length of heat tape needed to preheat the working fluid.

#### 3.3.1 Nomenclature

$A$  = area

$Cp_{air}$  = specific heat at constant pressure of cabin air

$\epsilon$  = emissivity

$\eta$  = fin efficiency

$F$  = View Factor

$H$  = enthalpy

$K$  = Thermal Conductivity

$\dot{m}$  = mass flow rate

$\dot{Q}$  = heat transfer rate

$\dot{Q}_{deposition}$  = heat transfer rate necessary for CO<sub>2</sub> deposition

$\dot{Q}_{cool}$  = heat transfer rate necessary to cool cabin air

$\dot{Q}_{total}$  = total heat transfer rate for the system

$\rho$  = density

$\sigma$  = Stefan-Boltzmann constant,  $\approx 5.67 * 10^{-8} \frac{W}{M^2 * K}$

$T$  = temperature

#### 3.3.2 Numerical Analysis with Python: Radiator Panel Size Analysis

For radiators, there is a positive correlation between the size of the radiator and the total heat rejection rate of the radiator. This can be noted by the inclusion fins in both convection-based radiators as well as thermal radiation-based radiators. The purpose of the fins is to increase overall surface area, as an increased area means an increased heat transfer rate. The equation for heat transfer rate via thermal radiation is below.

Eqn 1 
$$\dot{Q} = \epsilon * A_s * \eta * \sigma * F * (T_{surface}^4 - T_{surrounding}^4)$$

Determining the approximate size of the thermal radiator is incredibly important for being able to extrapolate experimental data to a real-world analysis of the function of the radiator. For the analysis, the above equation is used. The assumptions used are that view factor and fin efficiency are 1, the radiative plane is flat, the surrounding (sink) temperature is 4 K, and that the emissivity is 0.85. These assumptions are similarly used in the paper "Power Optimization of Cryogenic CO<sub>2</sub> Deposition Capture in Deep Space". [9] The goal of the analysis is to plot the necessary surface area of the radiator in relation to the surface temperature of the radiator and heat rejection rate. Plotting was performed in Python using the Matplotlib library.

Figure 9: Python Code for Plotting Panel Size

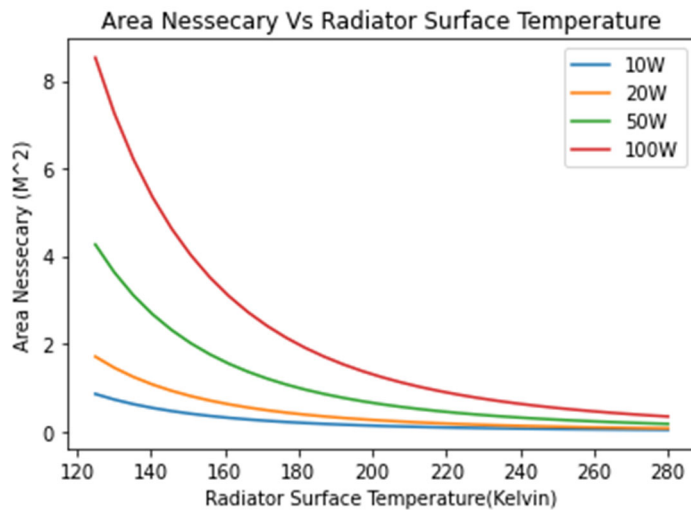


Figure 10: Relationship of Area, Temp, and Q

Figure 10 shows that as heat rejection rate increases and radiator temperature decreases, there is a sharp increase in the necessary size of the radiator.

### 3.3.3 Finding CO<sub>2</sub> Deposition Energy

The gas flow input (simulated) to our system is a gaseous mix of CO<sub>2</sub>, N<sub>2</sub>, and O<sub>2</sub>, at a total pressure of 760mmHg (1 ATM), flowing at 5 SLPM, at an average temperature of 295.5K (based on the ISS internal temperatures) and a CO<sub>2</sub> partial pressure of 2mmHg. This is below that of the 3mmHg on the ISS, for the purpose of crew safety. [10] The system is to remove 4.16Kg/day of CO<sub>2</sub> from the atmosphere of the cabin. The deposition temperature of

CO<sub>2</sub> is approximately 142K at the partial pressure of 2mmHg, however our system will achieve a deposition side temperature of 130K, as to have a temperature gradient between the gas and the radiator, as well as to be able to absorb heat through the deposited CO<sub>2</sub> that will accumulate through the process. To understand the amount of heat flow rate to be absorbed through the radiator, it must be calculated in two steps. First, we need to find what heat transfer rate is necessary to bring the entire 5 SLPM flow down to the temperature of 130K. Second, we need to find the heat transfer rate necessary to pull the latent heat of deposition of the CO<sub>2</sub> in the air out of that CO<sub>2</sub> to get the CO<sub>2</sub> to deposit on the side of the radiator. The sum of these two heat transfer rates will give us our total heat transfer rate. The equations and calculations below are used to calculate the total heat transfer rate necessary with the given input parameters.

Eqn 2 
$$\dot{Q}_{total} = \dot{Q}_{cool} + \dot{Q}_{deposition}$$

Eqn 3 
$$\dot{Q}_{cool} = \dot{m}_{cabin\ air} * C_{p\ air\ at\ 300K} * \Delta T_{air}$$

Eqn 4 
$$\dot{Q}_{deposition} = \Delta H_{CO_2\ deposition} * \dot{m}_{CO_2}$$

Eqn 5 
$$\dot{m}_{cabin\ air} = \rho_{air} * volumetric\ flow\ rate$$

Calculating mass flow rate of CO<sub>2</sub> in the system (Eqn 5):



$$\frac{5 \frac{\text{Liters of gas}}{\text{Minute}}}{22.4 \frac{\text{Liters}}{\text{Mol of ideal gas}}} * \frac{2 \text{mmHg of CO}_2}{760 \text{mmHg total}} * \frac{44.1 \text{ grams of CO}_2}{\text{Mol of CO}_2} = 0.259 \frac{\text{grams of CO}_2}{\text{minute}}$$

$$= 0.00000043 \frac{\text{Kilograms of CO}_2}{\text{second}}$$

Calculating mass flow rate of cabin air in the system (Eqn 5):

$$\dot{m}_{\text{cabin air}} = 1.194 \frac{\text{Kg of air}}{\text{m}^3} * 5 \frac{\text{Liters of air}}{\text{minute}} * \frac{1 \text{ minute}}{60 \text{ seconds}} * \frac{1 \text{ m}^3}{1000 \text{ liters}} = 0.00009946 \frac{\text{Kilograms of air}}{\text{second}}$$

Calculating heat transfer rate to cool cabin air to 130K (Eqn 3):

$$\dot{Q}_{\text{cool}} = 0.00009946 \frac{\text{Kilograms of air}}{\text{second}} * 1.006 \frac{\text{KJ}}{\text{Kg} * ^\circ\text{K}} * \frac{1000 \text{ Joules}}{1 \text{ Kilojoule}} * (295.5^\circ\text{K} - 130^\circ\text{K}) = 16.55 \text{ Watts}$$

Calculating heat transfer rate to deposit CO<sub>2</sub> (Eqn 4):

$$\dot{Q}_{\text{deposition}} = 571 \frac{\text{Kilojoules}}{\text{Kilogram}} * \frac{1000 \text{ Joules}}{\text{Kilojoule}} * 0.00000043 \frac{\text{Kilograms of CO}_2}{\text{second}} = 0.243 \text{ Watts}$$

The total heat transfer rate is the sum of the deposition and cool heat transfer rates (Eqn 2):

$$\dot{Q}_{\text{total}} = 16.55 \text{ Watts} + 0.243 \text{ Watts} = 16.793 \text{ Watts} \approx 17 \text{ Watts}$$

### 3.3.3 Numerical Analysis with Python: Equivalent Thermal Resistance

For the first design of the radiator, the number of pipes had to be balanced between being low enough that the NC gas doesn't impact the overall thermal resistance in capture mode, but high enough that the hot fluid flowing through could reject heat to the deposited CO<sub>2</sub> in recovery mode. It was noted from prior research of heat rejection with hot fluid flowing through pipes in a radiator, there is a point where the heat rejection increase per additional pipe had a drastic knee at about 23 pipes in their 2 meter wide radiator. [11] That is to say that they noticed a drastic knee in their chart of System Heat Rejection vs Tube Quantity per Panel at that point. However, there was no discussion about the use of NC gas and the thermal resistance as it compared to number of pipes. To analyze the thermal resistance of the piping system in capture mode, with NC gas filling the pipes, Python was used to plot graphs of thermal resistance vs number of pipes. The methodology of determining the equivalent thermal resistance of the piping setup was to redistribute the cross sectional area of the piping to two blocks of even cross sectional area to the original, and to place those blocks in either series or parallel to model the equivalent thermal resistance.

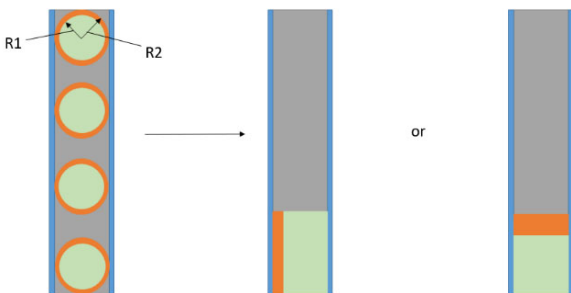


Figure 11: Single-Row Piping Config. Redistributed

Figure 11 shows the representative redistribution of a row of piping into series (middle) or parallel (right) configuration. Both series and parallel assumptions were made because the thermal conductivity of a static gas is many orders of magnitude lower than that of the piping material, so while heat would be more likely to tend to conduct through the pipe and around the gas, some heat would still travel through the gas. Because of this, the actual value of equivalent thermal resistance would be between that of the strictly parallel and strictly series assumption,

listing more towards the parallel assumption. The equation for equivalent thermal resistance via conduction is below.

Eqn 5 
$$\text{Equivalent Thermal Resistance}_{\text{conduction}} = \frac{\Delta X}{K \cdot A}$$

With these equations and methodology, a Python script was created to plot the equivalent thermal resistance compared to number of pipes. The program displayed the thermal resistance in the series assumption as the orange colored line in the attached graph and displayed the parallel assumption as the blue colored line. Figure 12 shows the code used. These blocks incorporate the libraries used and initialize variables for dimensions of the radiator and thermal properties of the radiator materials. Variable construction for the dimensions of the portioned components of the radiator as well as the series calculations for

Figure 12: Python Code for Thermal Resistance

resistance are compiled in blocks 3 and 4. Parallel calculations for resistance are compiled in block 7. Note that the suffix 'p' is used for parallel designation.

Figure 13 shows that a significant spike in thermal resistance occurs at between 60 and 80 pipes in the 1-meter by 1-meter model for the series assumption. Thermal resistance (units on this plot are K/W, Kelvin per Watt) for the parallel assumption model stays significantly lower as the number of pipes increases. This model does assume that the heat transfer is strictly one dimensional, with no heat moving in the direction from pipe to pipe or in the direction that the pipes move through the radiator. This model will be further refined as we progress in the design process to include multi-directional heat transfer as well as other configurations of pipes (such as for Rev 3, which has multiple rows of pipes divided by vacuum insulation).

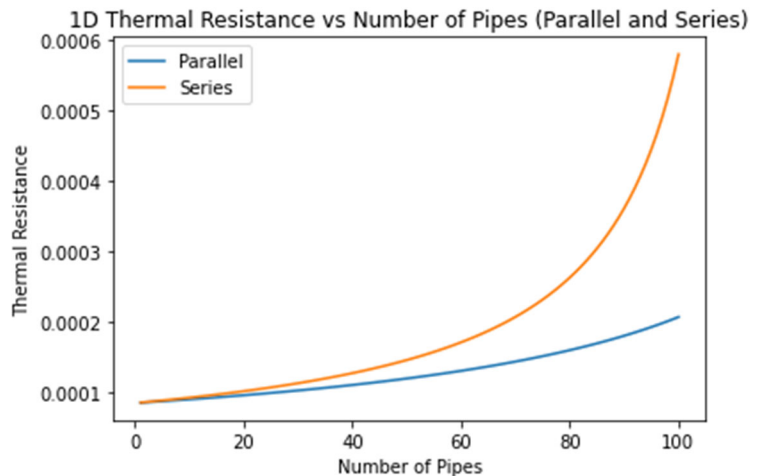


Figure 13: Plot for Series and Parallel thermal resistance

### 3.3.4 Solidworks FEA

For the Solidworks simulations, testing was initially done with a single panel out of the double panel radiator to determine the optimal working fluid flow rate for the system, to try to get the system to where the heat transfer between the panels most accurately mimics an actual system aboard a spacecraft during deep space transit. This testing showed that the working fluid flow rate has a drastic impact on the overall heat transfer through the system, and that incredibly small flow rates still move a great amount of heat. The chosen mass flow rate of Propylene for the system as determined to be .005 Kg/s, as this testing was done prior to the issues sourcing a cryogenic pump. Prior to that, inlet fluid temperature was modified to find the optimal balance between heat transfer through the system, achievable steady state

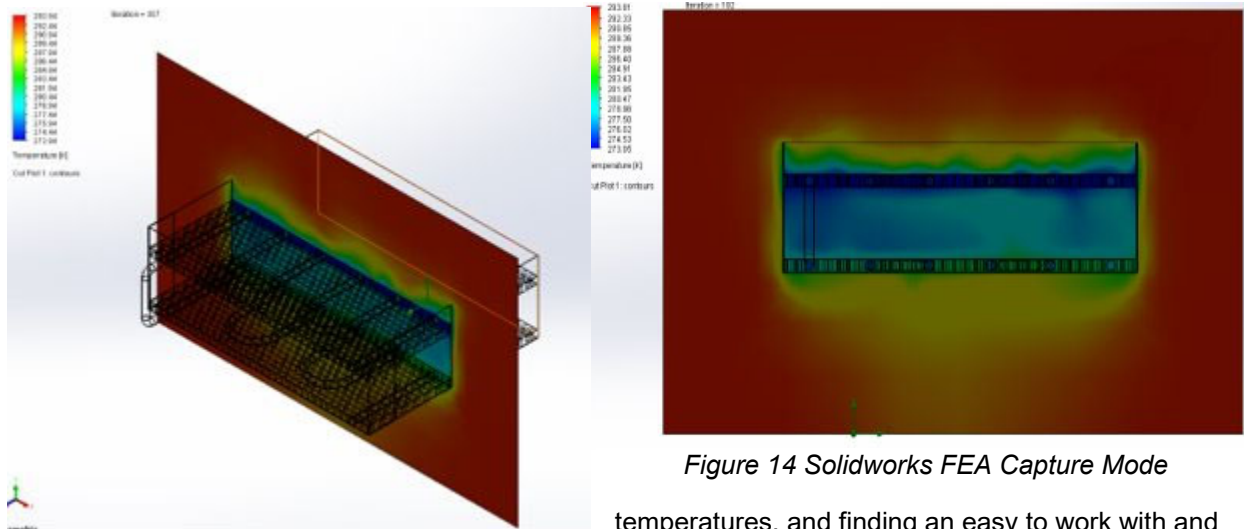


Figure 14 Solidworks FEA Capture Mode

temperatures, and finding an easy to work with and repeatable amount of power input to the system. Our testing determined that with the mass flow rate of .005 Kg/s, an Acetone inlet temperature of 210K provided a necessary heat input to the system of 91W, which is the power input we continued to use for the duration of the simulations. Acetone was used at this point because of the difficulties sourcing a cryogenic pump. For these tests, with the system decoupled, we determined the heat output from the cold panel first, to find the necessary heat input from the heater panel. This was done as it is significantly

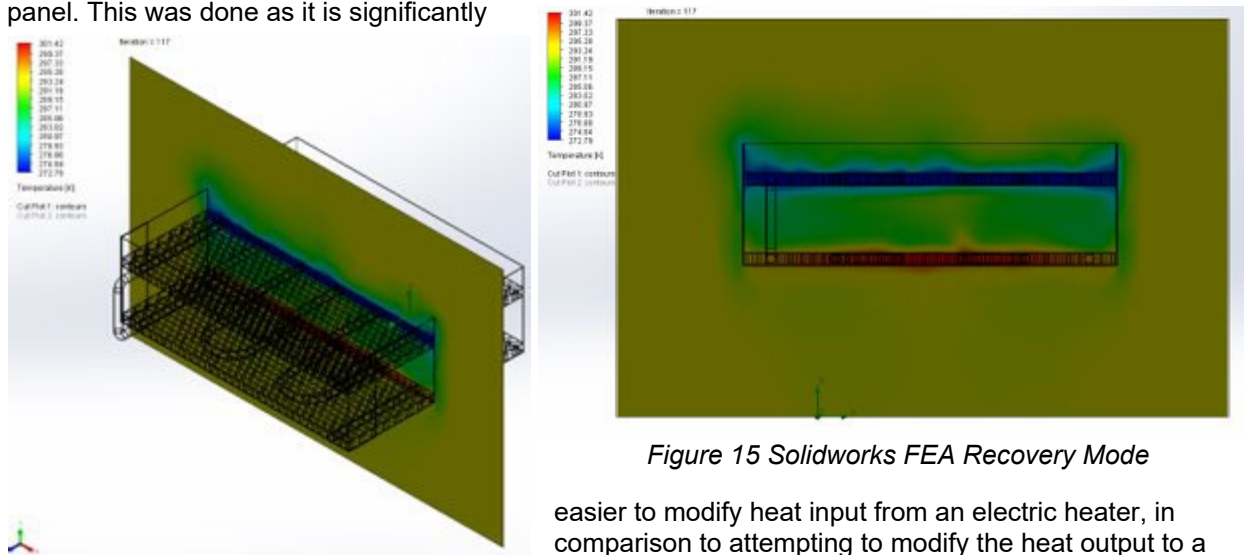


Figure 15 Solidworks FEA Recovery Mode

easier to modify heat input from an electric heater, in comparison to attempting to modify the heat output to a liquid heat sink. From this point, testing began with the full system in capture mode. Our initial tests with running the system in capture mode showed very odd results, we were getting a net heat output of the system of ~130W, which eclipses even our heat input of 91W. Our initial speculation was that with the system fully coupled, the total cross-sectional area of the

shell that heat could pass through was ~2.4in, and that this acted as a significant heat bridge between the heater and the heat sink. Multiple modifications were made to the midsection, including increasing the overall height of the midsection from 1.402in to 3in and altering the material to PVC, with a thermal conductivity of .16 W/m<sup>2</sup>\*K, but all to no avail. Switching the flow direction of the fluid, however, solved the issue. In the full, coupled test, we set the flow direction to have an inlet to the heater panel, and the outlet at after the heat rejection panel. This was opposite to the initial, decoupled tests, but it more accurately and directly showed us the direction of heat transfer. This flow direction, from heater to heat sink, resulted in a significantly higher ΔT between the fluid entering the heat rejection panel, and the isothermal boundary condition set as the liquid heat sink. This ΔT caused a significantly higher heat rejection from the fluid to the heat sink. Reversing the flow direction fixed this issue. From this point, we retested the model to determine the inlet temperature necessary to reach steady state, as with the thermal bridge of the outer shell, there was still a net heat output of the system. Steady state was determined to be reached at ~203K. From this, testing on Recovery mode began. With our initial 12x12 radiator design, the equivalent thermal resistance of the system was determined through multiple tests to be .33 °C/W. After this point, the model was updated to match the assembled testbench, and testing was done to verify the prior model results and update them with the new model. With the new model, with the .005 Kg/s inlet flow of Acetone, the Acetone dry ice bath heat sink, and 91W being input to the heater panel, steady state was reached at 202K. The decrease in temperature comes from a slightly larger radiator panel. The equivalent thermal resistance of the model in recovery mode was found to be .289 °C/W. Another important aspect of the design is that the overall ΔT between the face sheets in capture mode always lied between 7.5°C and 9.5°C.

In conjunction with Solidworks FEA, iterative process was used to determine many of the parameters used in the Solidworks FEA. This Excel spreadsheet is available in Appendix E.

### 3.3.5 Calculation for Heat-Tape

The following shows the calculation to find the proper length of pipe that would need to be wrapped with heat-tape. The heat-tape specified was an Omega 13 W/m<sup>2</sup>, 1 in wide, 8 ft long heat-tape. This condition is a constant heat flux condition, so this is the equation to be used. Mass flow rate was determined using Solidworks FEA, and Cp coefficient was determined to be 2 kJ/kg\*K.

$$\dot{q}A = \dot{m}c_p(\Delta T)$$

$$13 \frac{W}{m^2} * A = 0.005 \frac{kg}{s} * 2 \frac{kJ}{kg * K} (80K)$$

$$A = 61.5 in^2$$

$$L = \frac{61.5 in^2}{\pi(.5in)} = 39.18 in \sim 40 in$$

The area calculated is the total surface are of pipe to be covered. Since surface area of a cylinder is the circumference times the length, the L calculated represents the length of pipe that would need to be covered by heat-tape.

## 3.4. Safety Considerations

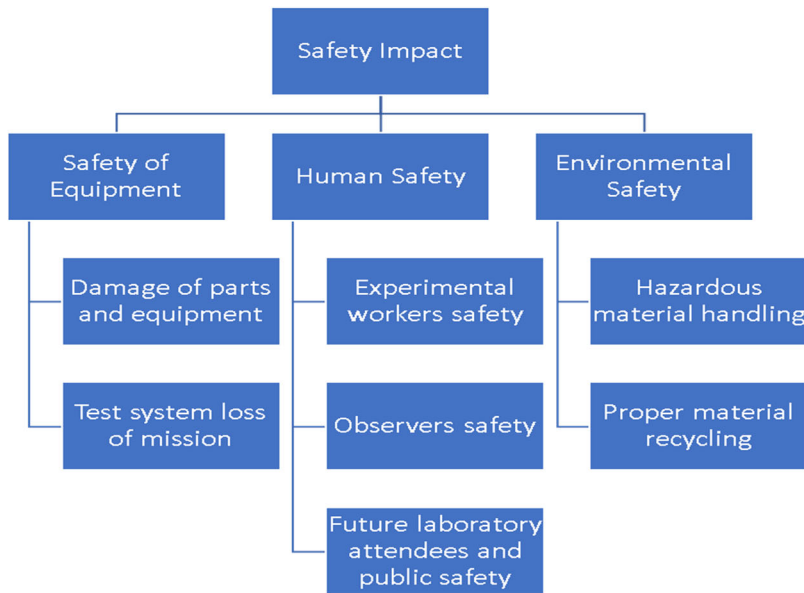


Figure 16: Safety Flow-Down

Safety in a laboratory environment is a top priority. In effort to put the safety of our team first, risks, consequences, and mitigation approaches to these risks have been identified. We have categorized safety into three main categories: equipment safety, human safety, and environmental safety (see Fig 13).

Many of the below safety considerations were written prior to the decision to use acetone-dry ice instead of liquid nitrogen. However, all of these considerations are left in this report because they still apply and because the system will be upgraded in the future by other researchers to accommodate liquid nitrogen.

### Safety of Equipment

We will ensure to use appropriate materials consistent with our analysis to construct our prototype in order to limit the possibility of failure due to material. To ensure the safety of the equipment, we will order parts that meet or exceed our specifications required. We will inspect incoming parts for obvious defects and check fitment prior to assembly.

Prior to testing and data acquisition, we will run the cycle with low pressures of gas and use a combination of soap and water to detect leaks. This ensures we can further test the thermal conductance radiator without any leaks in the system. Many of the liquids we may use in the radiator are harmful to bare skin and corrosive to equipment.

We will follow strict start-up and shut-down procedures every time we do any testing in order to safely operate the equipment and minimize the likelihood of damage to equipment, researchers, or the laboratory environment.

### START-UP

1. Initiate the software LabView VI, turn on all sensors and verify that they are reading.
2. Turn on pump without using liquid nitrogen for the “deep space” side, check for leaks ensure, plumbing is cycled correctly.
3. Introduce the cycling of the coolant via valve.
4. Once conditions are steady, cool “deep space” side with liquid nitrogen.

6. Initiate heater at certain temperature to simulate latent heat of CO<sub>2</sub> on deposition side and monitor.
7. Ensure temperature, flow rate, and pressure sensors are reading data as expected.

**SHUT-DOWN**

1. Turn off heater.
2. Stop cooling “deep space” side with the liquid nitrogen.
3. Turn off pump.
4. Purge coolant out of plumbing with NC gas via valve.
4. Ensure temperature, flow rate, and pressure sensors are reading data as expected.
5. Stop LabView VI, turn off sensors.

During testing we will be carefully monitoring temperatures, flow rates, and pressures to make sure our system is working correctly. Additionally, we will be dealing with temperatures as low as 90 K to simulate deep space via liquid nitrogen. Because of this, it is important we handle these materials with special gloves and aprons. In the event of an emergency, we will have system shut-off-switches wired at strategic locations to turn off pumps and to remove coolant/gas from the radiator. Following testing and collection of data, we must power down the system carefully in order to not rupture any pipes and potentially release any coolant. The coolant will be extremely cold and could cause freeze-burns as well as chemical burns to bare skin.

<b>Risk</b>	<b>Consequences</b>	<b>Mitigation Approach</b>
<b>Valve malfunction</b>	Affects the flow rate of the coolant and NC gas.	Prior filtration for radiator and constant monitoring.
<b>Pump failure</b>	System will stall.	Back up pump.
<b>Leakage of NC gas</b>	Pressure drops in the system.	Leak test system prior to cycling.
<b>Leakage of coolant</b>	Coolant may be toxic to environment as well as people involved in testing environment.	Leak test system prior to cycling.
<b>Excess pressure in radiator</b>	Pipe rupture and leakage of coolant.	Monitor pressure and purge as needed and use materials that will comply with associated pressures.
<b>Ice Burns</b>	Potential workplace injury.	Personal protective equipment and proper handling and training.
<b>COVID-19</b>	Health issues & project complications.	Social distancing, sanitation, and mask.

*Table 2: Risks, Consequences, and Mitigation Approach*

**Human Safety**

Human safety is the most important of the three categories. During testing of the prototype, we will make our safety and the safety of any other observers/researchers a top priority. We will ensure that only properly trained personnel operate the test systems and the liquid nitrogen systems. Any observers or other researchers will keep a safe distance from the testing area. All personnel will be equipped with the appropriate personal protective equipment, or PPE, as dictated by UNT laboratory policy and by the Occupational Health and Safety Administration (OSHA). [12] OSHA Hazardous Communication standard warning labels will be used on all test equipment in order to ensure hazards are clearly marked to personnel. These are some of the warning labels we may use:

<p>Gas Cylinder</p>  <p>• Gases Under Pressure</p>	<p>Warning of gases under high pressure. To be displayed on any pressure vessel.</p>
<p>Health Hazard</p>  <p>• Carcinogen • Mutagenicity • Reproductive Toxicity • Respiratory Sensitizer • Target Organ Toxicity • Aspiration Toxicity</p>	<p>Warning of harmful/toxic material. To be displayed on any harmful/toxic material.</p>
<p>Environment (Non-Mandatory)</p>  <p>• Aquatic Toxicity</p>	<p>Warning of material particularly harmful to aquatic life. To be displayed on any material particularly harmful to aquatic life.</p>
<p>Corrosion</p>  <p>• Skin Corrosion/Burns • Eye Damage • Corrosive to Metals</p>	<p>Warning of corrosive material, harmful to equipment or humans. To be displayed on any corrosive material.</p>
<p>Exclamation Mark</p>  <p>• Irritant (skin and eye) • Skin Sensitizer • Acute Toxicity (harmful) • Narcotic Effects • Respiratory Tract Irritant • Hazardous to Ozone Layer (Non-Mandatory)</p>	<p>General warning of material or equipment harmful to humans, environment, or equipment. To be displayed on any material or equipment that does not have a specific Haz Comm logo.</p>
	<p><b>Wear Safety Glasses</b> Prevent damage to eyes from harmful substances/dangerous equipment</p>
	<p><b>Wear Protective Gloves</b> Prevent damage from contact with extremely cold surfaces</p>
	<p><b>Wear Protective Clothing</b> Prevent damage from contact with extremely cold surfaces</p>


	<p><b>Wear Safety Shoes</b> Prevent damage to feet from falling objects, prevent slipping</p>
---	---

Table 3: OSHA Haz Comm Standards

The following table outlines the possible risks, consequences, and mitigation approach for Human Safety:

Risks to Human Safety	Consequences	Mitigation Approach
<b>Leakage of coolant</b>	Contamination of laboratory with harmful chemicals	Prior leak testing, stop system, containment of coolant, proper disposal while workers wear PPE.
<b>Excess pressure in pipes</b>	Pipe rupture and test system and prototype reconstruction	Use materials that meet or exceed pressures involved.
<b>NC gas leakage</b>	Mildly harmful contamination in lab	Ventilate lab environment, stop and purge system.
<b>Improper handling of liquid nitrogen</b>	Temperature of liquid nitrogen can cause severe ice burns, experiment must stop	Proper training and PPE while supervised

Table 4: Human Safety Risks, Consequences, Mitigation Approach

### Environmental Safety

Many of the chemicals we will be experimenting with are potentially harmful to the environment if not properly disposed of. Many of the substances we may choose from that are capable of maintaining liquid state at very low temperatures (as low as 90 K) are particularly harmful to aquatic life. After the testing is done, we will ensure we contain the fluids used and recycle/dispose of them responsibly.

## 3.5. Ethical/Professional Considerations

For this project, the human safety is the top priority. The radiator will be an integral part of the cabin air revitalization system. To meet NASA's requirements, we will go through multiple tests with the system to ensure a good concept of operations. Although this is not the final design that will be implemented into the spacecraft, it is still our ethical and professional duty to ensure the data we collect is able to be used by NASA for future development. In order to ensure our data is reliable, we will follow all ANSI, ASTM, and any other guidance & standards that are applicable.

Since liquid Nitrogen is potentially hazardous, we will be following ANSI CGA P12-2017, Safe Handling of Cryogenic Liquids, 6<sup>th</sup> ed. Additionally, we will follow ASTM B903-15, Standard Specification for Seamless Copper Heat Exchanger Tubes.<sup>1</sup>

We will also recognize the limitations of our testing environment, and only collect data that is repeatable through proper experimental controls. This will ensure that our data is as accurate and precise as possible. Any assumptions we make will be clearly defined.

<sup>1</sup> These are ANSI/ASTM documents we cannot yet reference at this time; they must be purchased



### 3.6. Estimated Life Cycle of Development

For the estimated lifespan of the designed testbench, with very few moving components, the testbench will not have many “weak links”. Small cryogenic pumps can last thousands of hours, such as the Cryomech AL300, which has a MTTF of 8000 hours [13]. Electric valves have a shorter lifespan, usually 1-3 years if well maintained [14], however, the cold temperatures for this project could pose issue to this component. Valcor manufactures cryogenic valves that they advertise as having a “long life”, but with no MFFT data or advertised lifespan. For piping, copper shows to be an excellent material for subzero temperatures with its high durability at cryogenic temperatures [15]. Propylene, a possible working fluid, is very stable in storage, however it does boil at well below room temperature, which can cause a loss of propylene to the atmosphere that would need to be replaced. 1-Butene is similar to propylene in that they both store stable but boil below room temperature and would need to be restocked if any is lost due to boiling. Thermocouple lifespans are widely ranging, as “thermocouple life expectancy varies greatly from just a few hours to many years.” [16] System maintenance and inspection should occur at least after every 24hrs of operation. Inspection should include ensuring no leaks have formed, no visible cracks have formed, that all pumps and valves are operational, and ensuring the function of sensors. With few overall moving parts in the proposed test bench design, with proper sensing equipment the test bench should be able to last far beyond the life of the project.

### 3.7. Cost Breakdown of Development

The following table itemizes materials and components to be purchased for manufacturing the prototype. Ideally, these materials and components will be purchased in phases, corresponding to the phases of manufacturing (to be determined). Most likely, items 1 through 5 will be in phase 1, as these are the items needed to build the main structure of the radiator. Next, we will order all valves, fittings, and sensors (items 6 through 8, and 13 through 17). Finally, the consumables, pump, and heater will be ordered (items 9 through 12, 18).

Item No.	Description	Quantity	Unit Cost (US\$)	Total Cost (US\$)	Vender
1	Polyethylene foam insulation for pipe 3/8", I.D. 1/2"	3			McMaster-Carr
2	Straight connectors, copper w/ center stops, 3/8" female ends I.D. 1/2"	12			McMaster-Carr
3	90-degree connectors, copper, 3/8" female ends, I.D.1/2"	12			McMaster-Carr
4	Copper pipe coil, 10 ft., 3/8", O.D. 1/2", I.D. 0.402"	4			McMaster-Car
5	Flush mount rivets, Aluminum (250 pack), dia. 1/8", length 0.212"	1			McMaster-Carr
6	Compressed air regulator (NC gas) w/ gauge & knob, 1/2 NPT	1			McMaster-Carr
7	Pressure safety valve, male inlet, 1/4 NPT-20 UNEF female relief port	1			McMaster-Carr
8	Copper brazing rods, pack of 10	2			McMaster-Carr

9	Brazing rings copper high strength, 10 pack, for pipe O.D. 1/2"	2	McMaster-Carr
10	Brazing flux, 0.5 lbs.	1	McMaster-Carr
11	Aluminum pipe coil, 10 ft, 3/8", O.D. 1/2", I.D. 0.402"	2	McMaster-Carr
12	3003 Aluminum Pipe, 6 ft. Straights, O.D. 1/2", I.D. 0.468"	2	McMaster-Carr
13	Copper Tubbing Coil 50 ft, OD 1/2" ID.402	2	McMaster-Carr
14	Honeycomb 3000 aluminum core, thickness 1/2", cell size 1/2", 24"x24"	2	McMaster-Carr
15	Copper piping straight, 6 ft., O.D. 1/2", I.D. 0.370"	2	McMaster-Carr
16	Copper Straight Connector Reducer for tube OD 1/2" to OD 1/4"	10	McMaster-Carr
17	Copper T Fitting OD 1/2" to 1/4"	5	McMaster-Carr
18	Check Valve 3/8" pipe, Female Ends, ID 0.675"	1	McMaster-Carr
19	Plastic Tank Reservoir, 2.5-gal capacity	1	McMaster-Carr
20	LOCTITE Structural Adhesive	3	McMaster-Carr
21	4-way valve, T-Pattern flow option, brass, 1/4" NPT Female ends	1	McMaster-Carr
22	NPT Reducer fitting male ends, brass, 1/4" to 1/8"	6	McMaster-Carr
23	NPT Reducer fitting male ends, brass, 3/8" to 1/4"	6	McMaster-Carr
24	NPT Reducer fitting male ends, brass, 3/8" to 1/4"	6	McMaster-Carr
25	0.05" Thick Aluminum sheet 3003-H14, 0.05" Thick, 24" x 24"	2	Online Metals
26	aluminum sheet 3003-H14, 0.05" Thick, 24" x 48"	3	Online Metals
27	Tape Heater, 1245 Watts, Heat Flux 13 W/in <sup>2</sup> , Length 8 ft, Width 1"	3	Omega
28	Voltage Converter, step up/step down, 110v to	1	Grainger

	220v AC, 220v to 110V AC 1.5kV VA Rating.		
<b>29</b>	Watlow Heater Width 6", length 10", Voltage 120V	1	Instrumart
<b>30</b>	Husky 4ft. Wood Top Work Bench	1	Home Depot

*Table 5: Bill of Materials*

## 4. FABRICATION

Fabrication took place over the course of 2 months utilizing D170 work area and F160 machine shop at UNT Discovery Park. Much of the work was done by hand utilizing various hand-tools. The following sections break down the fabrication methods and the stages of fabrication.

### 4.1. Fabrication Methods

Three main fabrication methods were used to construct the radiator: bending/forming, joining, and cutting/drilling.

#### 4.1.1 Bending & Forming of Coil Tubing & Sheet Metal

All bending of the copper tubing for the interior radiator panels was done by hand with a ½” tube bender. This device is comprised of two levers, a fulcrum, and a guide. The fulcrum provides a pivot point, while the two levers and the guide form the pipe to the desired bend.



Figure 17 Tube bender

As shown in the image to the left, the result is a neat, symmetrical u-bend. To facilitate the bend and ensure the piping does not kink, sand can be added to the inside of the pipe. This keeps the pipe walls from collapsing.

Other bending & forming methods included using the sheet metal bending machine at UNT. This machine is capable of neatly bending heavy gage sheet metal. This was used for forming the outer aluminum side panels (see image below). This simple machine works in similar fashion as the tube bender; sheet metal is placed in the slot on the machine and the two levers are pulled down, bending the aluminum sheets 90 degrees.



Figure 18 Sheet metal bender

#### 4.1.2 Joining Methods: Riveting & Brazing

Two main joining methods were used: riveting and brazing. Rivets are strong, lightweight fasteners and were most appropriate for this application over other methods like welding. Rivets are comprised of two parts: the shank and the mandrel. The mandrel (2) expands the shank (1), pulling the two objects being riveted together. Rivets are the most appropriate joining method for the aluminum panels of the radiator due to the expansion & contraction of the aluminum during thermal cycles. When testing the apparatus, we want the radiator to be able to expand & contract without warping or damaging. Rivets create a strong joint but also allow for some movement as the material expands & contracts. Also, they are lightweight which is desirable for space applications.



Brazing is a joining method similar to soldering. It is used for creating strong, durable, leak-proof connections between pipes and fittings. We chose brazing over other methods of joining pipes and fittings together due to the possibility of the extremely high pressures that could be encountered when turning the system off. When the system is shut off, the working fluid inside (initially propylene was selected) will heat up and expand. Brazing completely seals the joints and is extremely strong when done properly. Brazing works by heating up the pipe and fitting with an oxy-acetylene torch, and then melting silver alloy rods into the gaps between the fitting & pipe. For our application, brazing rods of 20% silver were used. 20% silver alloy rods are much more expensive, but provide a much stronger joint than brazing rods of lesser silver content.

*Figure 19 Brazing using silver alloy rod*

### 4.1.3 Cutting & Drilling

Various cutting and drilling devices were used. Electric hand drills were adequate for most of the drilling, and were particularly useful once the radiator was near complete (it would have been very bulky and hard to manage if we had put the entire radiator on a drill press). Hand drills were also useful for resetting rivets if they did not join properly or a mistake was made with them. An industrial sheet metal shear similar to the one picture below was used to cut all of the pieces of aluminum sheet metal prior to bending. Handheld reciprocating saws were also used for small cuts & various tasks.



*Figure 20 Sheet Metal Shear [21]*



Finally, the last cutting method used was a hand-held pipe cutter. Because copper coil tubing is so soft, it was easily cut using this device. The cutter works by rolling a hardened, sharp disk (2) around the diameter of the pipe. A screw (3) is used to slowly tighten the rollers (1) & cutting disk until it is all the way through the wall of the pipe.

Figure 21 Ridgid™ pipe cutter

## 4.2. Fabrication Stages

Fabrication was broken down into 3 key stages: bending/cutting, joining, and assembly.

### 4.2.1 Bending & Cutting

First, the copper coil tubing was bent to shape using the tube bender (see Fig 17 above). Next, the aluminum face-sheets and side panels were cut and bent using the sheet metal shear and the sheet metal bender. Once face sheets were cut and the coil tubing was bent to shape, the aluminum honeycomb was placed and cut to fit the empty spaces around the piping within the radiator. The individual pieces were then ready for drilling and joining via rivets. Brackets made from 0.50" square aluminum stock were cut to 0.75" long pieces. These brackets were used to rivet the face sheets to in order to sandwich the face sheets to the piping.



Figure 22 Cutting aluminum honeycomb

### 4.2.2 Joining

After all pieces were cut to proper dimensions, the pieces were marked for drilling. A drill press was used for small items that needed to be held with a vice for proper safety. Hand drills were used for applications where a drill press was impractical. Because the material we used was soft 3000 series aluminum, hand drills were more than adequate for any drilling application. The drill press was really only needed for the 0.50" square brackets. After all holes were drilled, the pieces were mock assembled to check tolerances of the holes. Nearly all holes lined up and the pieces were riveted together. Some holes needed to be re-drilled and some rivets were not engaged properly by mistake and had to be drilled out and re-done. However, once the two individual panels were complete and joined, the result was a very strong and sturdy radiator.



*Figure 23 Dual panel radiator joining & assembly*

After the radiator was complete, all of the fittings were brazed to the copper tubing, and the external copper tubing was bent to shape (again using the tube bender). The piping of the two individual panels was connected via 90-degree elbow fittings. Hose barbs were brazed onto the ends of the coil tubing to allow vinyl tubing to connect to the pump and the reservoir. This was done for the ability for the system to be disassembled if needed. Vinyl tubing will need to be replaced with copper coil tubing if the system is upgraded to handle liquid nitrogen. Because the heater tape and the heater for the bottom of the radiator did not arrive in time, the exposed copper plumbing was insulated with piping insulation foam.



*Figure 24 Brazing fittings to the piping system*

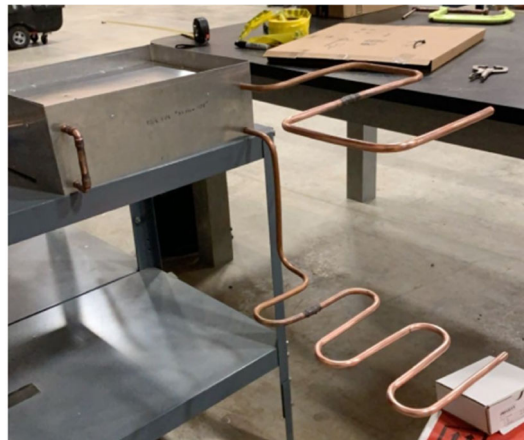


*Figure 25 Finished plumbing after brazing & bending*

### 4.2.3 Assembly

Assembly consisted of attaching all of the major components (radiator, pump, reservoir, and valves) together and attaching them to the workbench. A shelf was attached to the backboard of the workbench for the radiator to sit on. The pump was attached to a bracket on the workbench and set lower than the level of the fluid in the reservoir in order for better pump efficiency & less head loss. Vinyl tubing and hose clamps were attached to the hose barbs on the radiator external plumbing and connected to the fluid reservoir and to the pump. Vinyl tubing also connected the pump and the reservoir.

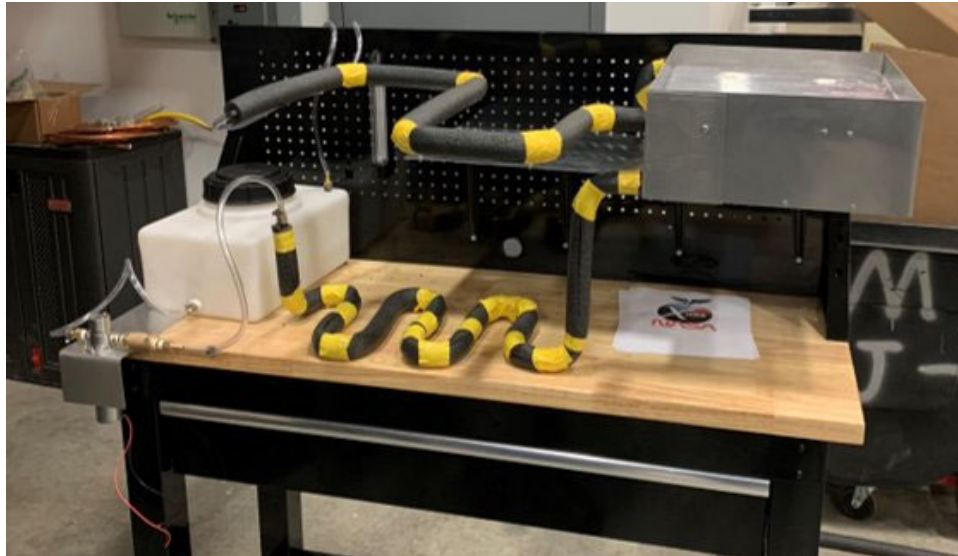


Figure 26 Fully assembled system, post-leak-check, prior to DAQ integration

Once all major components were attached, the system was leak-checked with water. An in-line filter was added between the reservoir and pump in order to protect the pump from the leftover metal shavings in the copper piping as a result of fabrication. No leaks were detected, and the system was then brought to the Thermal Management Lab in F180 of UNT Discovery Park to be connected to the data acquisition (DAQ) system. Nine thermocouples were attached to the system: four on the top of the upper radiator panel (heat sink or space side), four on the bottom of the lower radiator panel (CO<sub>2</sub> collection side), and the last one to the inlet of the pump in order to monitor the temperature of the fluid going into the pump.

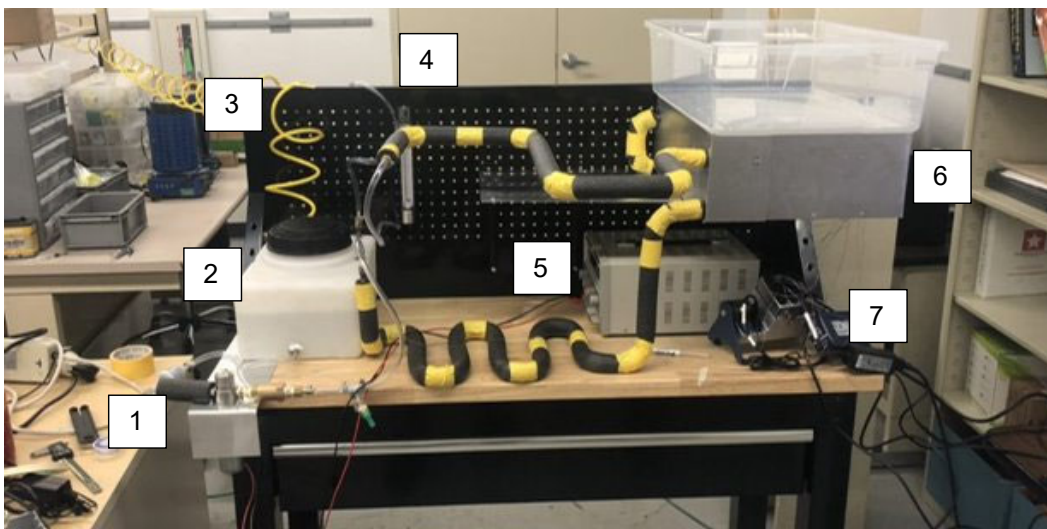


Figure 27 Fully assembled system, integrated with DAQ, prior to testing; 1) pump, 2) reservoir, 3) air line for purging system, 4) flow meter, 5) power supply unit for pump, 6) dual-panel radiator, 7) DAQ



## 5. TESTING

Testing was cut short due to time and resource constraints. We were able to leak-check the system, and see that the system is working and capable of collecting data, but we were not able to collect any data prior to the deadline for the project.

### 5.1. Testing Plan

The following steps outline the testing procedure.

1. Ensure reservoir is full of working fluid (at least 1.5 gal)
2. Turn on pump to 4.3 Volts (this is the required voltage for 0.300 L/min flow rate)
3. Let system run for 5 minutes, check for leaks
4. Add acetone to the ice bath area on top of the radiator
5. Using protective gloves and tongs, add several chunks of dry ice to the acetone
6. Monitor the bath regularly & add dry ice as needed
7. Allow system to reach steady state (est. 30-45 minutes)
8. Once steady state has been reached, let system run for 15 minutes.
9. Turn off pump
10. Connect air to T-fitting
11. Remove lid to reservoir  
[NOTE] This step is vital to ensure reservoir does not rupture from the compressed air
12. Slowly turn on air, setting regulator to 10 psi
13. Wait for the fluid to be completely evacuated, then let run for an additionally 5 minutes to ensure all fluid has been removed
14. Turn off the air, disconnect & re-cap the T-fitting
15. Replace lid to reservoir.
16. Stop DAQ software, save data as Excel

Acetone dry-ice with a working fluid of acetone will be used for the actual test, but the system will be leak-check and pre-tested with water and an ice water bath.

### 5.2. Instrumentation and Data Acquisition

For data acquisition (DAQ), National Instruments CompactDAQ modules and LabVIEW software were used. Thermocouple wires were placed at 9 key points on the system to monitor the temperatures on the face sheets and the temperature of the working fluid going into the pump in order to protect the pump if the working fluid was too cold.

Four thermocouples were placed on top, on the “space” side or recovery side of the radiator. Four more were placed on the bottom, or CO<sub>2</sub> capture side. The final thermocouple was placed at the inlet of the pump. This was done to be able to monitor the fluid temperature and turn off the pump if the fluid was too cold. An analog sapphire ball flow meter was placed between the radiator and reservoir to monitor the flow rate.

The flow meter was calibrated by setting the pump to a certain voltage, and measuring/weighing how much water was pumped in 60 seconds. Since 1 liter of water equals 1 kg of weight, we were able to find the flow rate for a corresponding voltage and reading on the flow meter. This was accomplished for 2 different voltages, then a linear equation was determined to find the voltage for a certain flow rate, since flow rate and voltage increase linearly.

<i>Voltage</i>	<i>Flow Meter Reading (mm)</i>	<i>Flow Rate (L/min)</i>
2.5 V	63 mm	0.123 L/min
3.0 V	85 mm	0.173 L/min
4.3 V	147 mm	0.316 L/min

*Table 6 Flow Meter Calibration/Testing*

$$v = 10(\dot{V}) + 1.27$$

This equation was used to determine the voltage needed for a flow rate of 0.300 L/min. 0.300 L/min requires a voltage of 4.27 volts. Since the power supply unit used only had one decimal place to it, the closest voltage of 4.3 volts was used. This led to an actual flow rate of about 0.316 L/min.



Figure 28 Weighing water to find volume, comparing to output of flow meter

### 5.3. Results

Due to time constraints, issues involved with our design and last-minute changes, we were not able to obtain any results. We were able to run the system to check for leaks, and see on the DAQ that the thermocouples were working. The plumbing of the system did not leak, but the ice-bath tub of the radiator was not water-tight and thus leaked ice water during our initial pre-testing with ice water and water as a working fluid. Our plan to work around this issue in the future is to coat the ice-bath tub with thick aluminum foil or to seal the cracks with a sealant capable of handling  $-80^{\circ}\text{C}$ . Another option is to simply place dry ice on the tub without acetone. The downside to this option is that the cooling would be non-uniform across the face sheet. Lastly, we have also considered buying gel-packs capable of being cooled to  $-80^{\circ}\text{C}$ , cooling them down, and placing these on top of the face sheet.

We were able to see on the DAQ display that there was a significant  $\Delta T$  from the top face sheet to the bottom. Additionally, we saw that the temperatures were changing as a result of the fluid circulating through the system.

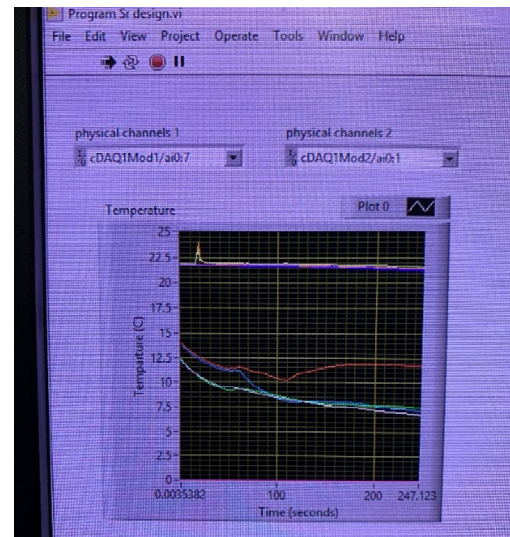
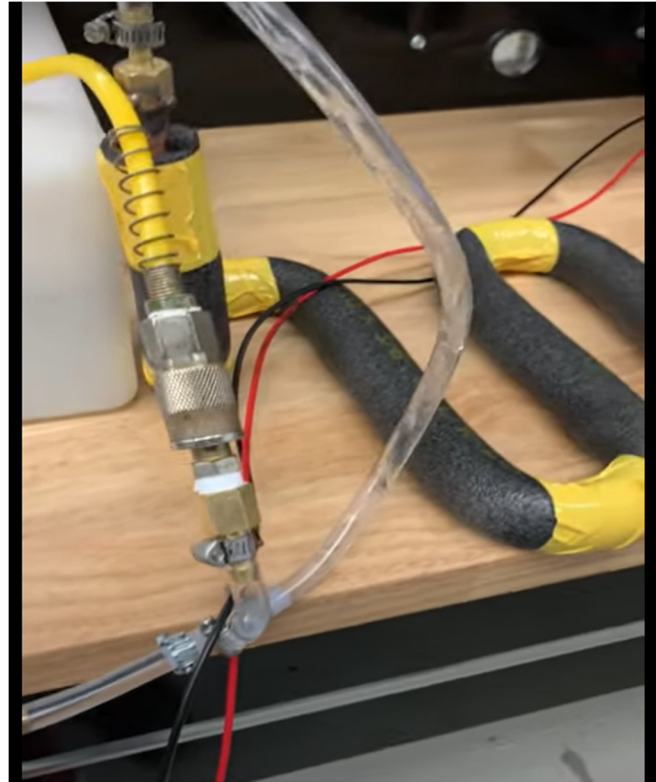


Figure 29 Screen capture of the DAQ with system on

Additionally, we were able to successfully clear the working fluid from the system. This procedure worked flawlessly; the check valve prevented the compressed air from going into the pump and reservoir from the wrong direction, and the fluid was quickly and completely evacuated. In Figure 29, air can be seen clearing the tubing to the right of the T-fitting, while air did not pass the check valve and so did not enter the tubing to the left of the T-fitting.

## 5.4. Conclusions

Although we did not finish testing, and we did not gather any data, our system still showed very promising results. We were able to see a temperature gradient across the radiator, and see that gradient start to change as the fluid circulated during our pre-test. We were able to successfully clear the system and go from capture mode to recovery mode. We have presented a viable, working proof-of-concept for the proposed academic innovation idea, and have set the framework for future students and researchers to continue the project. Although the system was changed to being used with acetone and dry ice, it can easily and quickly be upgraded to run with boiling liquid nitrogen and propylene should the proper pump be acquired. The entire system is simple, scalable, reliable, and cost-effective. Furthermore, it weighed in total under 20 lbs. Therefore, this variable conductance thermal radiator design is believed to be of great use to NASA for future research and projects, and potentially offer a viable option for future long-duration crewed space flights to the moon and beyond.



*Figure 30 Air purging the system & turning system to "capture" mode*

## 5.5. Additional Work Done during Summer 2021

A no-cost extension has been requested to continue to work on the project during summer 2021. However, due to the major HVAC renovations taking place at UNT Discovery Park, the Thermal Management Lab was not available for use most of the time, and only a limited set of preliminary experiments were conducted during the second half of August 2021. In these tests, water was used as working fluid, and ice-water bath was utilized as the constant temperature bath simulating heat sink. Sample data from the preliminary tests are presented in Figures 31-32.

Data in Figure 31 demonstrate the radiator operation in the capture mode. In this test, system circulated 0.07 LPM water flow rate through the radiator panels. Heaters applied a total of 1340 W heat into the CO<sub>2</sub> deposition surface and an ice-water bath provided constant-temperature heat sink on the heat rejection surface. Average temperatures from multiple thermocouples at the CO<sub>2</sub> deposition and heat rejection surfaces, as well as temperatures of the working fluid at the radiator inlet and outlet, indicate steady-state system operation over several minutes. Nearly identical working fluid temperatures at the inlet and outlet of the radiator suggest the heat added into the radiator on one side (simulating CO<sub>2</sub> deposition) was rejected out from the opposite side (simulating heat transfer to deep space). During steady state, there was approximately 20°C temperature difference across the radiator surfaces showing the low thermal resistance aimed in capture mode.

Data in Figure 32 demonstrate the radiator operation in the recovery mode. Before beginning this test, air was used to purge the water from the tubing in radiator, and then stagnant air was maintained inside the tubing during the test to effectively change the thermal conductance of the radiator. In this test, with a

heat load of 2750 W, steady-state conditions were not reached as can be noticed from the increasing temperatures, especially on the CO<sub>2</sub> deposition surface. Nevertheless, the data shows a much higher temperature difference (>55 °C) across the radiator surfaces demonstrating the high thermal resistance aimed in recovery mode.

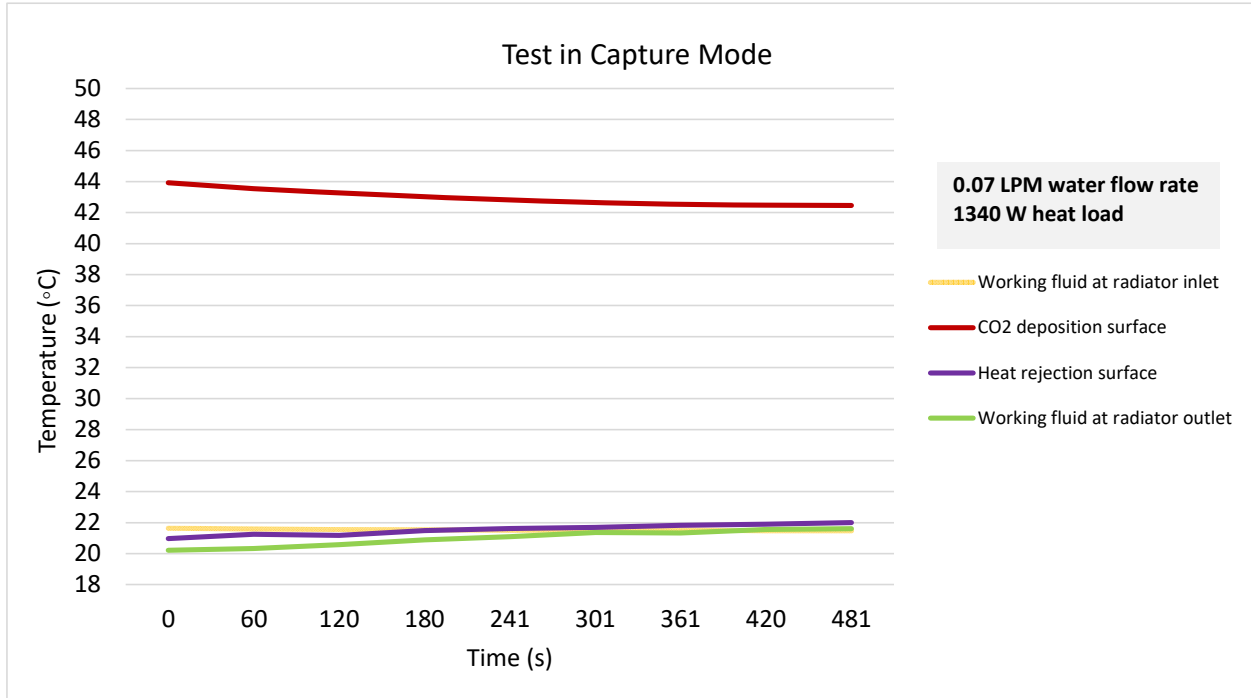


Figure 31 Preliminary testing of radiator prototype in capture mode

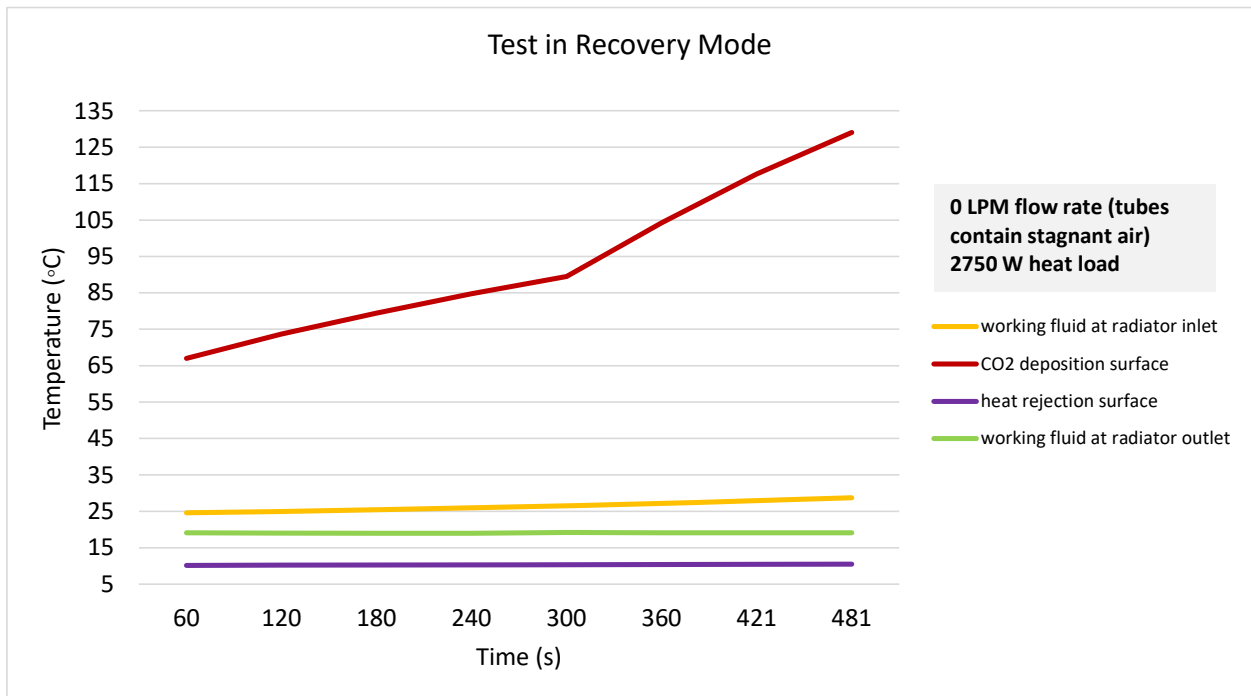


Figure 32 Preliminary testing of radiator prototype in recovery mode

## 6. MARKETING PLAN

Because of the nature of this project being an academic innovation challenge, and not a product that will be used by a company in the private sector to be sold or to generate revenue, a traditional marketing plan does not apply. However, a key part of our involvement in the X-Hab Academic Innovation Challenge is to communicate what we are doing to potential future participants by way of presenting our work to local high schools and science clubs. This will inform these students that they may very well have the opportunity to work hand-in-hand with NASA in the near future as a college student. Our project could motivate young minds and lead to today's students becoming tomorrow's NASA engineers & researchers.

Additionally, our findings might be presented at relevant conferences such as International Conference of Environmental Systems (ICES) conference. This will allow disseminating our work to industry leaders and experts.

### 6.1. Project Logo

This logo, designed by Eric Lira, incorporates 3 elements: the eagle, representing UNT, the X-Hab logo, representing the X-Hab Academic Innovation Challenge, and the NASA logo. Both the eagle and the NASA logo are "retro" logos, representing how our past is sending us forward into the future. The path set by the Mercury, Gemini, and Apollo programs is the foundation upon which we are expanding the technology to send mankind even further into the cosmos. This is the purpose of X-Hab – to broaden and deepen the technology needed to send man further than ever before.

## 6.2. Brochure

# Thermal Radiator for CO2 Deposition in Deep Space Transit

Sponsor: NASA

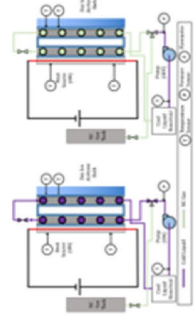
COLLEGE OF ENGINEERING  
Department of  
Mechanical Engineering

### Abstract

This UNT Senior design team was tasked by NASA to develop a variable conductance thermal radiator for CO2 deposition for deep space transit. Air revitalization is a crucial system for any space travel, be it for Low Earth Orbit, such as the International Space Station, or for deep space transit. Current systems, such as the Carbon Dioxide Removal Assembly aboard the ISS, require upkeep and maintenance, which cannot be done on long distance space missions. For the past several years, NASA has done research on Cryogenic systems for Carbon Dioxide removal. These systems operate on the idea that Carbon Dioxide freezes at a higher temperature than the air in the cabin atmosphere, which degrades over time. Current cryogenic systems are reliable but require significant energy input to operate. The goal of this project is to determine the effectiveness of a variable conductance physical thermal radiator that can reject heat to deep space, without the use of a dedicated heat pump to remove energy from the cabin air.

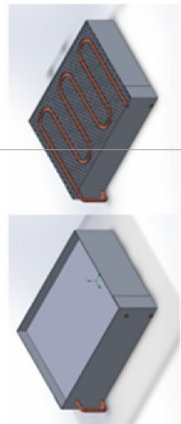
### Background/Design

As previously mentioned, the fundamental principle of operation for this design is that Carbon Dioxide freezes at a higher temperature (~-143°C) than Oxygen (~-218°C) and Nitrogen (~-209°C). The current leading method to reduce a portion of the cabin atmosphere to such low temperatures is by means of Sterling Cryocoolers. These advanced heat pumps are able to reach these extremely low temperatures, but they require a significant amount of electrical power to do so. The system we are designing will use a pumped liquid to perform the heat transfer of the thermal energy from the cabin atmosphere to deep space, which will only require a pump and a small electric heater to be electrically powered. When the pump is turned on in our system, fluid moves through two separate panels of our radiator, from one to the other. One of the panels is facing the section of the cabin designed to deposit the frozen CO2 on, and the other panel is facing space, with gas as cold as -269-15°C. Each panel has 5 parallel tubes, and the tubes are connected to a manifold. The manifold is designed to be empty, so as to minimize heat transfer through it. The fluid dumps heat to deep space, and then goes to the other panel, where it picks up thermal energy from the freezing of Carbon Dioxide. This cycle continues for as long as you wish to freeze out Carbon Dioxide. To remove the frozen Carbon Dioxide, a non-condensable gas is piped through the system, essentially "turning off" the radiator, and significantly reducing the overall heat transfer of the system. Removing frozen CO2 also requires an electric heater, however the power draw from the electric heater is over an order of magnitude lower than that of the Sterling Cryocooler.




### Methodology/Manufacturing

The initial design revisions were driven by means of Solidworks flow modeling. We used Solidworks to determine what specific parameters of the design affected the heat transfer coefficient overall of the radiator, and from those results we modified those parameters to achieve our specific heat transfer goals.



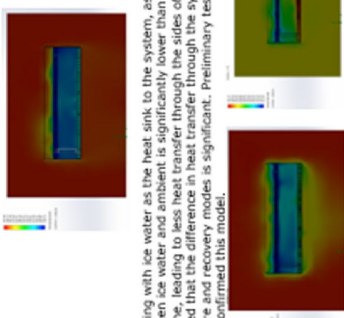
Solidworks also allows us to be able to test the system in a multitude of different situations and with a multitude of boundary conditions, some of which are unattainable on Earth. The tested conditions included flow rates, the main boundary condition that we can't attain here is the heat transfer by means of thermal radiation to a heat sink temperature of 4K (-269.15°C). This boundary condition is what the actual system, if implemented, will operate with. Knowing how the system operates under those conditions is extremely important to this project. An important component of the manufactured design is the use of heaters and a pre-cooler in order to pump the fluid. With concerns about acquisition of a cryogenic pump, we created the system to be able to use a heater prior to the pump and a chiller after the pump, to essentially create a pocket of significantly warmer fluid that most pumps can handle. The cooler is used after the pump to keep the fluid entering the system at the same temperature as the fluid exiting the system, so the system will function exactly the same as if a cryogenic pump was used.

Manufacturing of this project took place in D170 at UNT's Discovery Park. This process involved cutting material, bending pipes, brazing piping, drilling, etc. The full radiator system was placed on a workbench that allowed us to keep the system contained and set up in a manner that allows the system to be upgraded with components that can handle cryogenic temperatures, should a pump that can handle those temperatures be acquired.

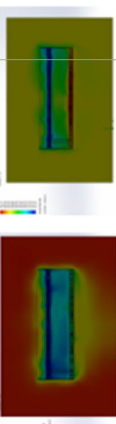


### Modeling Results

For the modeling of possible testing conditions, we used Solidworks flow modeling to achieve the results. For the condition of a dry ice acetone bath (195K) as the heat sink, 91W being applied to the deposition side, with acetone being pumped through the system at 0.005 Kg/s with a flow direction going through the sink side then the heater side, the system reaches steady state at a fluid temp of 202K and a deposition side temperature of 202.942K. This gives a change in temperature through the radiator of 7.942K, and with the goal being as minimal of a change in temperature through the radiator, we consider that a success. In recovery mode, with Nitrogen filling the piping with a flow velocity, with the dry ice bath at 195K, the change in temperature through the radiator is 10.1K. The goal in this mode is to "turn off" the radiator, so the higher the change in temperature through the radiator, the better.



Modeling with ice water as the heat sink to the system, as the delta T between ice water and ambient is significantly lower than that of dry ice and acetone, leading to less heat transfer through the sides of the system, showed that the difference in heat transfer through the system in the capture and recovery modes is significant. Preliminary testing with ice water also confirmed this model.



### References/Acknowledgements

Jagtap, P., Belanick, G., Jan, D., Hall, S., & Chen, W. (2020, July 31). *Power Optimization of Cryogenic CO2 Deposition Capture in Deep Space Deposition Subscale System Design and Test*.

Belanick, G., Jan, D., & Huang, R. (2019, July 7). *Spacecraft Carbon Dioxide Deposition Subscale System Design and Test*.

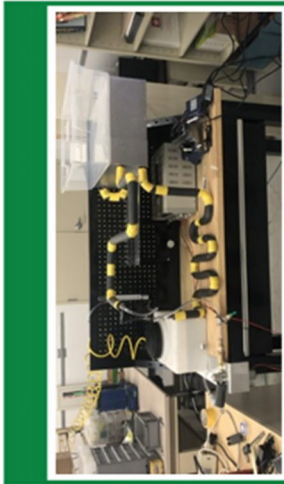
Many thanks to Dr. Huseyn Bostano, Dr. Cable Kurwitz and Baltimore Giron for their guidance & mentorship. Thanks to Mr. Bobby Grimes and Mr. Rick Pierson, for their help getting us the tools and machines we needed. Thank you to NASA and the great people we worked with for providing us this wonderful project and opportunity. Specifically, thanks to the NASA X-432-2022-1000-0000-0000 Challenge, the NASA Ames Cryogenic Deposition Systems (AES) Division Life Support Systems, the NASA-AMES Research Center. Finally, thank you to our sponsors Ms. Grace Belanick, and Dr. Darrel Jan of NASA.

Figure 33 Tri-fold Brochure, Inside



COLLEGE OF ENGINEERING  
Department of  
Mechanical Engineering

*I know the sky's not the limit,  
because there's footprints on the  
moon.  
-Buzz Aldrin*



**Team 9**

Front row: Jesus De La Torre (left), Eric Lira  
Back row: Anthony Pezulli (left), Travis Seaver

**2020-2020 M2M X Hab  
Academic Innovation Challenge**

Figure 34 Tri-Fold Brochure, Outside

### 6.3. Target Market

Our main target market is local high school students and science clubs/organizations. As participants in the X-Hab Academic Innovation Challenge, it is our duty to participate in educational outreach to these local students in the hopes of motivating future generations toward STEM career fields. [8]

Potential entities that might be interested to our project could include other government agencies and private sector companies such as Lockheed, Boeing, Northrup-Grumman, etc.

### 6.4. Means of Accessing the Target Market

Because of the difficulties with doing anything in-person due to the COVID-19 pandemic, accessing our target markets will most likely be completely online via Zoom, Facebook, and other online resources.

For the outreach program for local high schools, the original procedure was to visit local college/career days and science fairs, and to invite local educators to attend testing sessions we conduct. Since these events are most likely not going to happen any time soon, we can set up virtual demonstrations of our test sessions via Zoom. The following table includes local educators who have agreed to participate in demonstrations so far.

<b>Educator Name</b>	<b>High School/Department</b>	<b>Level of Involvement</b>
<b>Mrs. Barbara Urban</b>	Whitesboro High School/ Science Dept Head	Zoom w/ entire class, Date TBD

*Table 7: Educational Outreach POC's*

Once our tri-fold brochure is complete, we will also pass out this document electronically to local high schools and science clubs for them to further disseminate to their students/members.



## 7. TEAM PERSONNEL

Our team is a diverse group of highly motivated STEM students of multinational and multicultural backgrounds. Over half of the team is comprised of underrepresented minority students, including Hispanic-Americans and a Disable Veteran. As a Hispanic Serving Institution, UNT's focus on diversity allows us to better represent the demographic population of North Texas, which will allow our outreach program to local future STEM students to be more effective. Our diversity has also enhanced our creativity and our wide range of backgrounds has enabled us to problem solve in ways that might otherwise have not been possible.

### 7.1. Team Personnel Responsibilities

#### **Jesus De La Torre – Business Development & Marketing Lead**

***Callsign: “Toro”***

In his role on the X-Hab team, Jesus oversees all business development and marketing, including the team budget, the community outreach program to local high schools and science clubs, and assists with the CAD modeling of the prototype.

#### **Eric Lira – Testing & Prototype Development Lead**

***Callsign: “Cowboy”***

In his role on the X-Hab team, Eric oversees the development of the test prototype, to include identifying the specifications of materials & components, overseeing the Bill of Materials (BOM) & Purchasing Orders (PO's), and ensuring the safety of the testing environment.

#### **Anthony Pezzulli – Research, Analysis, and Design Lead**

***Callsign: “Godfather”***

In his role on the X-Hab team, Anthony quarterbacks research tasks, leads the team in calculations and analysis for the development of accurate models, and helps the team apply these models to the design of the prototype. Although already comfortable with computer programming, Anthony taught himself Python in the span of 1 week in order aid the team in numerical analysis.

**Travis Seaver – Project Manager & Manufacturing Lead**

***Callsign: “Beater”***

Travis is the team’s project manager and is the manufacturing lead. Under this title, he is responsible for the overall project timeline, modeling of prototype design, and overseeing the manufacture of the prototype as well as inspection/quality assurance of the finished product.

## 7.2. Resumes

[Next four pages]

---

---

---

---

---

---

---

---

---

---

---

---

---

---

---

---

---

---

---

---

---

---

---

# APPENDIX A:

## References

- [1] R. Hollingham, "Apollo in 50 numbers: The workers," 19 June 2019. [Online]. Available: <https://www.bbc.com/future/article/20190626-apollo-in-50-numbers-the-rocket>.
- [2] Y. A. Cengel and A. J. Ghajar, *Heat and Mass Transfer Fundamentals & Applications* (6th ed.), New York: McGraw Hill, 2020.
- [3] J. Isobe, P. Henson, A. MacKnight, S. Yates and D. Schuck, "Carbon Dioxide Removal Technologies for U.S. Space Vehicles: Past, Present, and Future," in *46th International Conference on Environmental Systems*, Vienna, 2016.
- [4] W. Raatschen, C. Matthias and H. Westermann, "Advanced Life Support System for CO<sub>2</sub>, H<sub>2</sub>, CO, R134a and VOC Removal on Submarines," in *47th International Conference on Environmental Systems (ICES)*, Charleston, 2017.
- [5] C. Marshall, "In Switzerland, a giant new machine is sucking carbon directly from the air," 1 June 2017. [Online]. Available: <https://www.sciencemag.org/news/2017/06/switzerland-giant-new-machine-sucking-carbon-directly-air>.
- [6] C. Song, Y. Kitamura, S. Li and W. Jiang, "Parametric Analysis of a Novel Cryogenic CO<sub>2</sub> Capture System Based on Stirling Coolers," *Environmental Science and Technology*, vol. 46, p. 12735–12741, 2012.
- [7] G. Belancik, D. Jan, R. Huang, J. Paredes-Garcia and J. Chambliss, "Characterizing Cryogenic Carbon Dioxide Capture for Life Support Systems," in *47th International Conference on Environmental Systems*, Charleston, 2017.
- [8] H. Bostanci and C. Kurwitz, "M2M X-Hab 2021 Academic Innovation Challenge: THERMAL RADIATOR FOR CO<sub>2</sub> DEPOSITION IN DEEP SPACE TRANSIT," University of North Texas; Texas A&M University , 2020.
- [9] P. Jagtap, G. Belancik, D. Jan, W. Chen and S. Hall, "Power Optimization of Cryogenic CO<sub>2</sub> Deposition Capture in Deep Space," in *50th International Conference on Environmental Systems*, Virtual, 2020.
- [10] G. Belancik, D. Jan and R. Huang, "Spacecraft Carbon Dioxide Deposition Subscale System Design and Test," in *49th International Conference on Environmental Systems*, Boston, 2019.
- [11] J. R. Miller, G. C. Birur, G. B. Ganapathi, E. T. Sunada and D. F. Berisford, "Design and Modeling of a Radiator with Digital Turn-Down Capability under Variable Heat Rejection Requirements," in *41st International Conference on Environmental Systems*, Portland, 2011.
- [12] "OSHA Hazard Communication Standard Pictogram," US Dept of Labor, 1 June 2015. [Online]. Available: [https://www.osha.gov/Publications/HazComm\\_QuickCard\\_Pictogram.html](https://www.osha.gov/Publications/HazComm_QuickCard_Pictogram.html). [Accessed 29 November 2020].
- [13] M. L. Alvarez, "THE DEVELOPMENT OF A CRYOGENIC OVER-PRESSURE PUMP," July 2012. [Online]. Available: <https://lss.fnal.gov/archive/masters/fermilab-masters-2012-03.pdf>. [Accessed 02 December 2020].

- [14] M. D'Amato, "To repair or replace?," 26 September 2010. [Online]. Available: <https://www.flowcontrolnetwork.com/valves-actuators/article/15554240/to-repair-or-replace>. [Accessed 02 December 2020].
- [15] W. M. M. a. F. F. C.A. Thompson, "Cryogenic Properties of Copper," National Institute of Standards and Technology (NIST), July 1990. [Online]. Available: <https://www.copper.org/resources/properties/cryogenic/>. [Accessed 02 December 2020].
- [16] A. Volbrecht, "GUIDELINES FOR GOOD THERMOCOUPLE PRACTICE," *HEAT TREATING PROGRESS*, pp. pp 48-51, May/June 2007.
- [17] J. Chambliss, J. Sweterlitsch and M. J. Swickrath, "Potential Uses of Deep Space Cooling for Exploration Missions," in *42nd International Conference on Environmental Systems (ICES)*, Houston, 2012.
- [18] J. C. Knox, "Development of Carbon Dioxide Removal Systems for NASA's Deep Space Human Exploration Missions 2017-2018," in *48th International Conference on Environmental System*, Albuquerque, 2017.
- [19] G. Belancik, D. Jan and R. Huang, "Analysis of Spacecraft Cabin Carbon Dioxide Capture via Deposition," in *48th International Conference on Environmental Systems*, Albuquerque, 2018.
- [20] National Aeronautics & Space Administration (NASA), "NASA Procedural Requirements," 09 November 2009. [Online]. Available: [https://nodis3.gsfc.nasa.gov/main\\_lib.cfm](https://nodis3.gsfc.nasa.gov/main_lib.cfm).
- [21] N/A, "Tennsmith Sheet Metal Foot Shear," Midwest Technology Products, [Online]. Available: <https://www.midwesttechnology.com/tennsmith-sheet-metal-foot-shear-60-x-80/>. [Accessed 19 April 2021].



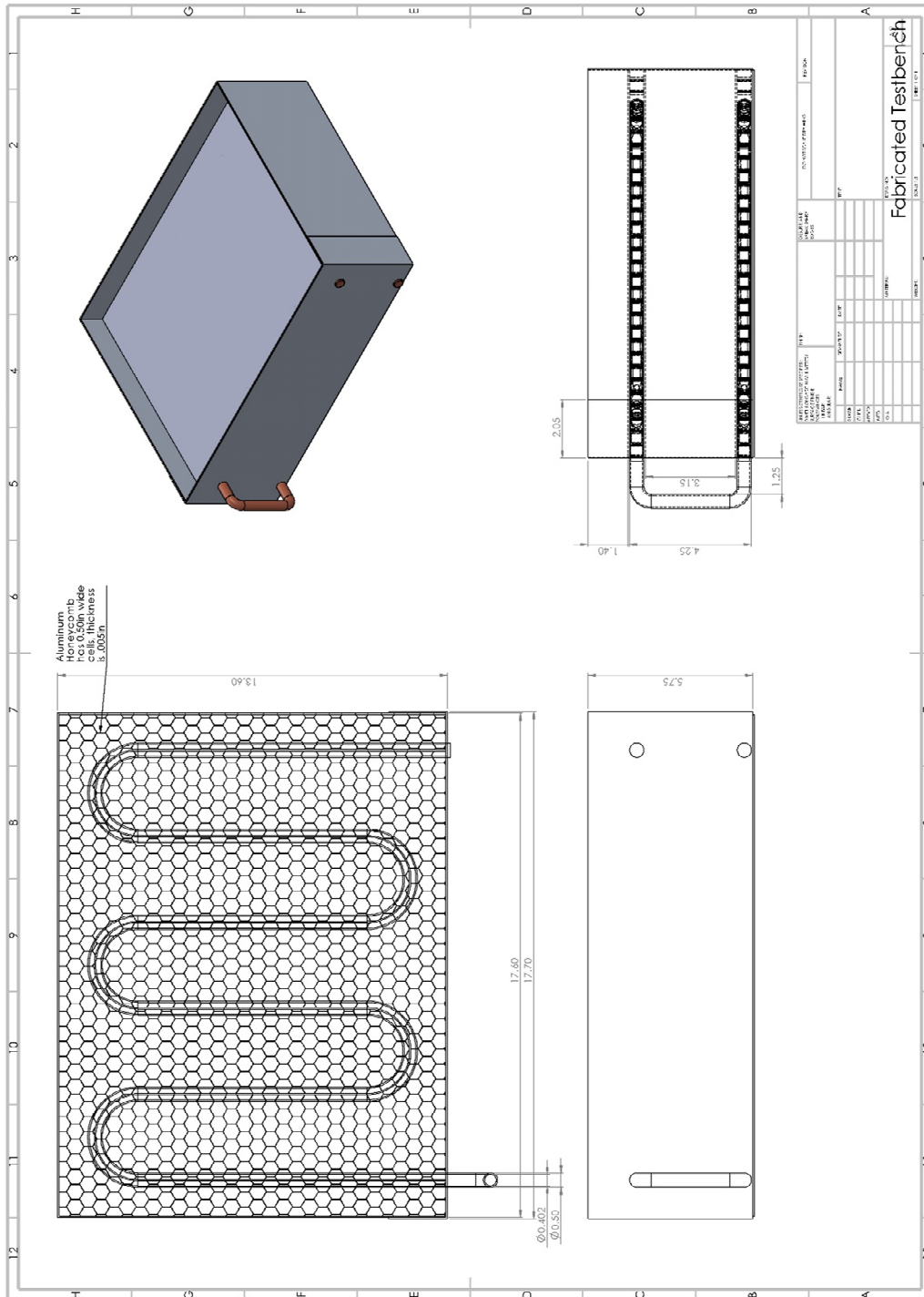
## APPENDIX B:

### Complete Specifications for Major Purchased Parts/Components

Item	Dimensions	Properties	Quantity	Item Number	Unit Cost (US\$)	Cost After Discount/Shipping (US\$)	Vender
Copper Pipes	Length 10 Ft, O.D 0.5", I.D 0.402"	K=385W/mK	3	8955K141			McMaster-Carr
Resevior	2.5 Gal	Plastic	1	4439T11			McMaster-Carr
Honeycomb Aluminun Core	Thickness: 0.5" Cell Size 0.5" 24"x24"	K=205 W/mK	2	9635K3			McMaster-Carr
Aluminium Sheets 3003-H14	Thickness: 0.05" 24" X 48"	K=205 W/mK	3	8089			McMaster-Carr
Surface Thermocouple Probes	3/8" Lg. 1/16" dia.	-325F to 650F	2	9251T71			Lab Donated
Pressure Sensors	2.5" and 3.5" dials	1% accuracy	2	PGS-25L-100			Lab Donated
In-Line Flow Meters	7" long	5% accuracy	1	FL-505			Lab Donated
Gear Pump	1.2 lbs 3.1"x 1.75"	12 or 24 V DC, 3000 RPM	1	DGM09			Lab Donated
Check Valve	3/8" body, NPT Female Ends, ID 0.675"	Brass body	1	47715K22			McMaster-Carr
Copper Connector	for 3/8" pipe, ID: 0.5"	Max Pressure 150 PSI	10	5520K143			McMaster-Carr
Watlow Heater	6"x10"	120V	1	060100C1-0001B			Instrumart

# APPENDIX C:

## Drawings for Custom-Built or Fabricated Parts/Components/Sub-Assemblies



## APPENDIX D:

### Bill of Materials

Item No.	Description	Quantity	Unit Cost (US\$)	Total Cost (US\$)	Vender
1	Polyethylene foam insulation for pipe 3/8", I.D. 1/2"	3			McMaster-Carr
2	Straight connectors, copper w/ center stops, 3/8" female ends I.D. 1/2"	12			McMaster-Carr
3	90-degree connectors, copper, 3/8" female ends, I.D.1/2"	12			McMaster-Carr
4	Copper pipe coil, 10 ft., 3/8", O.D. 1/2", I.D. 0.402"	4			McMaster-Carr
5	Flush mount rivets, Aluminum (250 pack), dia. 1/8", length 0.212"	1			McMaster-Carr
6	Compressed air regulator (NC gas) w/ gauge & knob, 1/2 NPT	1			McMaster-Carr
7	Pressure safety valve, male inlet, 1/4 NPT-20 UNEF female relief port	1			McMaster-Carr
8	Copper brazing rods, pack of 10	2			McMaster-Carr
9	Brazing rings copper high strength, 10 pack, for pipe O.D. 1/2"	2			McMaster-Carr
10	Brazing flux, 0.5 lbs.	1			McMaster-Carr
11	Aluminum pipe coil, 10 ft, 3/8", O.D. 1/2", I.D. 0.402"	2			McMaster-Carr
12	3003 Aluminum Pipe, 6 ft. Straights, O.D. 1/2", I.D. 0.468"	2			McMaster-Carr
13	Copper Tubbing Coil 50 ft, OD 1/2" ID.402	2			McMaster-Carr
14	Honeycomb 3000 aluminum core, thickness 1/2", cell size 1/2", 24"x24"	2			McMaster-Carr
15	Copper piping straight, 6 ft., O.D. 1/2", I.D. 0.370"	2			McMaster-Carr
16	Copper Straight Connector Reducer for tube OD 1/2" to OD 1/4"	10			McMaster-Carr

17	Copper T Fitting OD 1/2" to 1/4"	5	McMaster-Carr
18	Check Valve 3/8" pipe, Female Ends, ID 0.675"	1	McMaster-Carr
19	Plastic Tank Reservoir, 2.5-gal capacity	1	McMaster-Carr
20	LOCTITE Structural Adhesive	3	McMaster-Carr
21	4-way valve, T-Pattern flow option, brass, 1/4" NPT Female ends	1	McMaster-Carr
22	NPT Reducer fitting male ends, brass, 1/4" to 1/8"	6	McMaster-Carr
23	NPT Reducer fitting male ends, brass, 3/8" to 1/4"	6	McMaster-Carr
24	NPT Reducer fitting male ends, brass, 3/8" to 1/4"	6	McMaster-Carr
25	0.05" Thick Aluminum sheet 3003-H14, 0.05" Thick, 24" x 24"	2	Online Metals
26	aluminum sheet 3003-H14, 0.05" Thick, 24" x 48"	3	Online Metals
27	Tape Heater, 1245 Watts, Heat Flux 13 W/in <sup>2</sup> , Length 8 ft, Width 1"	3	Omega
28	Voltage Converter, step up/step down, 110v to 220v AC, 220v to 110V AC 1.5kV VA Rating.	1	Grainger
29	Watlow Heater Width 6", length 10", Voltage 120V	1	Instrumart
30	Husky 4ft. Wood Top Work Bench	1	Home Depot

# APPENDIX E:

## FEA Parameters Iterative Analysis

One Panel, backside, air in honeycomb, Al Pipes	Inlet Flow Rate (kg/s)	Inlet Temp (K)	Outlet Temp (K)	Inlet Pressure (Pa)	Outlet Pressure (Pa)	Head Loss (Pa)	Power Added	Power to fluid (W)	Power efficiency to pipes (%)	Op. Fail
	0.05	204.56	212.706	99827.5	99827.5	639		143.7141	99.1427333	2017
Full System, flow from heater to heat sink	Inlet Flow Rate (kg/s)	Inlet Temp (K)	Outlet Temp (K)	Inlet Pressure (Pa)	Outlet Pressure (Pa)	Head Loss (Pa)	Power Added	Power to fluid (W)		Op. Fail
	0.05	210	186.527	99796	99796	601		-185.77025		2017
Full System, no air	Inlet Flow Rate (kg/s)	Inlet Temp (K)	Outlet Temp (K)	Inlet Pressure (Pa)	Outlet Pressure (Pa)	Head Loss (Pa)	Power Added	Power to fluid (W)		
	0.05	210	186.024	99827.5	99827.5	501.7		-133.27146		
Full System, 3in mid section, with air	Inlet Flow Rate (kg/s)	Inlet Temp (K)	Outlet Temp (K)	Inlet Pressure (Pa)	Outlet Pressure (Pa)	Head Loss (Pa)	Power Added	Power to fluid (W)		
	0.05	210	187.456	100283	100283	340		-427.92174		
Full System, no air, 3in of PVC for midsection (0.16 W/m <sup>2</sup> )	Inlet Flow Rate (kg/s)	Inlet Temp (K)	Outlet of heater panel	Inlet Pressure (Pa)	Outlet Pressure (Pa)	Head Loss (Pa)	Power Added	Power to fluid (W)		
	0.05	210	213.171	100330	100330	9975		-104.29955		
Full System, no air, decoupled	Inlet Flow Rate (kg/s)	Inlet Temp (K)	Outlet of heater panel	Inlet Pressure (Pa)	Outlet Pressure (Pa)	Head Loss (Pa)	Power Added	Power to fluid (W)		
	0.05	210	213.171	100330	100330	9975		-104.29955		
Full System, no air, 3in of PVC for midsection (0.16 W/m <sup>2</sup> ), flow from cold to hot	Inlet Flow Rate (kg/s)	Inlet Temp (K)	Outlet Temp (K)	Inlet Pressure (Pa)	Outlet Pressure (Pa)	Head Loss (Pa)	Power Added	Power to fluid (W)		
	0.05	210	207.037	99823.1	99823.1	-441.9		-23.81125		
Full System, with air, 3in of PVC for midsection (0.16 W/m <sup>2</sup> ), flow from cold to hot	Inlet Flow Rate (kg/s)	Inlet Temp (K)	Outlet Temp (K)	Inlet Pressure (Pa)	Outlet Pressure (Pa)	Head Loss (Pa)	Power Added	Power to fluid (W)		
	0.05	210	205.243	99840	99840	-525		-427.93145		
Full System, with air, 3in of PVC for midsection (0.16 W/m <sup>2</sup> ), flow from cold to hot	Inlet Flow Rate (kg/s)	Inlet Temp (K)	Outlet Temp (K)	Inlet Pressure (Pa)	Outlet Pressure (Pa)	Head Loss (Pa)	Power Added	Power to fluid (W)		
	0.05	207	205.504	99557	99557	-525		-15.00716		
Full System, with air, 3in of Al for midsection, flow from cold to hot	Inlet Flow Rate (kg/s)	Inlet Temp (K)	Outlet Temp (K)	Inlet Pressure (Pa)	Outlet Pressure (Pa)	Head Loss (Pa)	Power Added	Power to fluid (W)		
	0.05	207	205.241	99836.5	99836.5	-525.5		-37.409515		
Full System, with air, 3in of Al for midsection, flow from cold to hot	Inlet Flow Rate (kg/s)	Inlet Temp (K)	Outlet Temp (K)	Inlet Pressure (Pa)	Outlet Pressure (Pa)	Head Loss (Pa)	Power Added	Power to fluid (W)	Delta Face Sheet	
	0.05	205	201.191	99858.2	99858.2	-423.8		-102.24756	203.175	1176
Full System, with air, 3in of Al for midsection, flow from cold to hot	Inlet Flow Rate (kg/s)	Inlet Temp (K)	Outlet Temp (K)	Inlet Pressure (Pa)	Outlet Pressure (Pa)	Head Loss (Pa)	Power Added	Power to fluid (W)	Delta Face Sheet	
	0.1	220	208.091	105655	105655	-505.1		-106.821	208.107	1176
One Panel, cool side, 220K Acetone working fluid, 155K isothermal panel, air in honeycomb, Al Pipes	Inlet Flow Rate (kg/s)	Inlet Temp (K)	Outlet Temp (K)	Inlet Pressure (Pa)	Outlet Pressure (Pa)	Head Loss (Pa)	Power Added	Power to fluid (W)	Heater Face Temp	
	0.01	220	210.364	106122	106122	1011.9		1943.5312	5063	2038.5853
	0.01	220	203.353	100257	100257	100245		112	234.91599	276.5307
	0.005	220	204.56	100259	100259	100237		52	151.6784	164.795895
	0.003	220	204.605	100256	100256	100236		30	93.155145	101.124312
One Panel, cool side, Acetone working fluid, 155K isothermal panel, air in honeycomb, Al Pipes	Inlet Flow Rate (kg/s)	Inlet Temp (K)	Outlet Temp (K)	Inlet Pressure (Pa)	Outlet Pressure (Pa)	Head Loss (Pa)	Power Added	Power to fluid (W)	Heater Face Temp	
	0.005	210	200.925	100231	100231	100226		55	91.531375	101.124312
	0.005	205	198.733	100270	100270	100220		50	63.202695	74.1031
	0.005	203	197.94	100277	100277	100218		59	51.0301	61.0301
Full system, Al, 3 in midsection, CO2 in pipe, recovery mode	Power to bottom	Top Temp	Bottom Temp	Delta T	Thermal Resistance	Needed Power				
	91	195	225.239	30.239	0.332296703	120.374351				
Full system, Al, 3 in midsection, CO2 in pipe, recovery mode	Power to bottom	Top Temp	Bottom Temp	Delta T	Thermal Resistance	Needed Power				
	120	195	234.551	39.551	0.329925	138.403418				
Full system, PVC 3 in midsection, CO2 in pipe, recovery mode	Power to bottom	Top Temp	Bottom Temp	Delta T	Thermal Resistance	Needed Power				
	91	195	275.306	84.306	1.99273925	20.07655565				
Testbench Model	Power to bottom	Top Temp	Bottom Temp	Delta T	Thermal Resistance	Needed Power				
	91	195	221.3	26.3	0.28940969	138.403418				